Chapter 2
Nanostructures Obtained Using Electric Discharges at Atmospheric Pressure

Pavel Topala, Alexandr Ojegov and Veaceslav Ursaki

Abstract The results of theoretical and experimental investigations of physical phenomena that accompany the formation of oxide and hydroxide nano-metric pellicles on metal surfaces by applying pulsed electrical discharge machining (PEDM) are presented. The chemical composition of the processed surface determined by Energy Dispersive X-ray analysis (EDX) attests the presence of oxygen that reaches the abnormal ammounts (up to 60 % at.) for all investigated alloys. The surface phase analysis using X-ray Photoelectron Spectroscopy (XPS) allows one to affirm that the oxygen in film forms three basic structures: $-O^{2-}$ (oxides), $-OH^{-}$ (hydroxides) and structures of C–O and O–C=O types. Experimental investigations have shown that the surface active resistance of these pellicles increases by about 10^7 times, the potential of corrosion increases to positive values and the speed of corrosion decreases in the chemically active media. Oxide pellicle formation occurs on flat, round and combined interior and exterior piece surfaces made of metal materials. It can be applied in oxide pellicle formation on piece surfaces aiming at providing anticorrosive protection; in surface passivation of construction pieces used in the chemical industry; in manufacturing active resistances of high values (10^6 Ω) and small dimensions (1 × 1 × 0.01 mm) used in microelectronics; in the production of elements with electronic emission surfaces.

2.1 Introduction

In recent decades, great attention is given to research related to the technologies of manufacturing low-dimensional objects such as nano-films, nano-particles, nano-wires and nano-tubes. With the reduction in size of new structures formed

P. Topala (✉) · A. Ojegov
"Alecu Russo" Balti State University, Balti, Moldova
e-mail: pavel.topala@gmail.com

V. Ursaki
Institute of Electronic Engineering and Nanotechnologies D. Ghitu,
Academy of Sciences of Moldova, Chisinau, Moldova

using novel technologies, some new electrical, mechanical, optical and chemical properties are formed and this is mainly the result of surface and quantum confinement effects. Low-dimensional objects represent a class of multifunctional materials very promising for application in machine and equipment building technology, microelectronics, photonics, medicine, chemical and biological sensors, etc. [1–4]. To emphasize the importance of low-dimensional objects it is sufficient to refer to nano-pellicles [2] and nano-wires which, as demonstrated recently [1, 5, 6], have unique thermal and electrical properties.

The formation of nano-metric oxide pellicles [7] on the active piece surfaces has found a rather wide application aiming at increasing resistance to wear and corrosion in pieces used in machine building, as well as at changing electrical conductivity properties for pieces in electronics and microelectronics.

Surface oxidation methods that use concentrated sources of energy such as plasma get, ion beam, electron beam, photon beam [8–19] have low efficiency of energy use and require the use of complicated equipment which is very costly. In case of formation of oxide layers in the electrolytic plasma, [9, 10] before anodizing, pieces subjected to processing require prior cleaning, degreasing and washing of the work surface. The thickness of oxide strata in the case of using this method is between units of micrometers to hundreds of micrometers. Harmful aqueous solutions of acids are used. The formed oxide pellicles possess porosity within the limits of 10–40 %. When the oxide pellicles are formed via the electric arc [20–23], the plasma get directed towards the processing surface causes partial melting of the surface layer; the oxide films are fragile and have poor adhesion with the base material subjected to machining; the process requires large expenditures of energy (for gas ionization, thermal and light radiation). All these methods do not solve the problem of nano-metric pellicle formation; the formed layers are fragile, spongy and develop roughness; further processing is necessary and special processing environments are required, etc.

The method of oxide nano-pellicle formation by applying pulsed electrical discharge machining (PEDM) is currently less known. The abnormal dissolution of oxygen in piece surfaces made of steel was attested for the first time [23], after which a series of works [7] attested the possibility of oxide and hydroxide pellicle formation in the amorphous state on metal surfaces.

An analysis of works [24–27] made it possible to conclude that generators of RC type with parallel priming can be successfully used for micro- and nano-oxidation of piece surfaces made of electrically conductive materials. Research on the interaction of PEDM plasma channel with electrode surfaces has shown that two types of interactions are characteristic of the electro-erosion phenomenon: type I—the appearance of "cold" electrode spots on the electrode surfaces which appear on the asperities and impurities from them [24–27] and cause surfaces clean of impurities, as well as thermal interaction with them, causing structural changes in the surface layers at small depths (in terms of nano- and micrometers); type II—after the "cold" electrode spots, the "hot" electrode spots are formed on the electrode surfaces; this causes essential melting of the processed surfaces, accompanied

by the phenomenon of vaporization and removal of electrodes' material in the form of drops [7, 25].

By analyzing the results obtained by the author of works [28, 29] it was stated that to obtain an interaction of type I with the plasma channel on the piece surface it is necessary that the energy density on the machined surface to be lower than the specific heat of material melting, and the latter can be expressed by the relation [28–35]:

$$\frac{4W}{\pi d_c^2 \cdot S} < Q_{melt} = q\rho, \tag{2.1}$$

where q and ρ are the heat of fusion and the density of piece material respectively; W is the energy emitted in the gap, d_c is the diameter of the plasma channel and S is the gap value.

As can be seen from (2.1), in the case when the energetic processing regime, the size of the gap and the thermo-physical properties of the piece material are known, it is possible to determine the diameter of the plasma channel which coincides with the size of its trace on the machined surface.

If we name the coefficient of trace overlap $k = 0.5$–$0.1.0$ and the frequency of pulsed electrical discharges f, then the technological process productivity may be determined by the relation:

$$\eta = \frac{k\pi d_c^2 f}{4} \tag{2.2}$$

It was demonstrated in [35, 36] that when applying PEDM for superficial processing, the erosion processes combined with melting and explosive vaporization of the electrode material occur for the most studied metals and alloys at durations of current pulses of 10^{-6} s. It follows that to achieve the expected effects it is necessary to ensure discharge pulses of relatively short duration.

The effects that take place on the electrode surfaces depend on the way of piece connection in the discharge circuit (as cathode (direct) or as anode (inverted)). These desiderates have been studied in [32] and it was established that for short duration pulses they are "cathode" and for long duration pulses they are "anode"— so in the case of superficial thermal treatment the piece will be included as circuit cathode. In the case of thermal treatment of steel pieces, their hardness increases by 2–0.3 times and in those of titanium surfaces it increases by 2–0.5 times at the depths of the formed layers from a few micrometers up to several tens of micrometers. The depth of these layers achieves the maximum value after three passes for steel and after five passes for titanium alloys [37, 38].

The interaction of plasma channel with the piece-electrode surface does not always have a pure thermal character, but often the work piece surface is enriched with elements from the environment where plasma forms and with the content of anode-tool material.

The depth of penetration of these elements in the piece surface layer depends on both the pulse energy and the size of the gap and can be expressed by the relation [29]:

$$h = \frac{kW_S}{AS},$$ (2.3)

where $W_S = \int_0^\tau U(t)I(t)dt$ is the energy emitted in the gap at a solitary discharge; U and I are the voltage on the gap and the current intensity in it respectively; τ is the pulse duration; A is the area of the surface attacked at a discharge; S is the gap value; k is a constant that depends on the thermo-physical properties of the processed material.

It has been experimentally proven that the surface oxidation is more effective when the work piece is connected in the discharge circuit as cathode (direct connection), because there are craters on the anode surface that are formed when the dielectric is pierced at its interaction with PEDM plasma.

An oxide film of a certain thickness, stable and adherent to the surface of the metal of origin, compact, continuous and free of pores or cracks can considerably slow down the development of the corrosion process. The condition for the film protection can be expressed by the coefficient of expansion [29–33] indicating the ratio between the volume of oxide and the volume of metal in the machined surface [39]:

$$\frac{V_{oxide}}{V_{metal}} > 1.$$ (2.4)

Surface oxidation is easy to achieve by applying PEDM. The materials subjected to processing can be conductive materials (metals and alloys), as well as semiconductor surfaces. The thickness of the oxide layer is counted in terms of nanometers, the environment is not contaminated and the ozone is formed, but the research concerning the functional properties of formed films made by the authors of works [32–36, 40–50] only scientifically ascertained the new effects.

2.2 Physical Model of Nano-Pellicle Formation by Applying Pulse Electrical Discharge Machining

Since the application of *PEDM* in technological purposes for dimensional machining [9, 19], the formation of deposits from compact and powder materials [7], as well as the micro-metallurgical processes that occur in the surface layer of the work piece were studied both in liquid and solid state. It was established that the formation of a new alloy in the machined surface is accompanied by convective

mixing of the components in the liquid phase and by the diffusion of elements in substrate from solid phase of deposition. It was shown that for the gaps bigger than 0.03 mm the interaction of PEDM plasma channel with the machined surface is manifested by the appearance of a trace consisting of a central zone that presents a crater with liquid phase and a zone of thermal influence of the freshly pickled metal color [22]. The central zone disappears for certain values of the gap and the machined surface presents only the zone of thermal influence, where phenomena of hardening and enriching the piece material with elements from the active media occur.

The priming voltage of pulsed electrical discharges depends on the gap value S and the pressure of gas P, and it is described by the relation of Paschen [7] that can be interpreted on the basis of Taundsen theory of breakdown. According to this law, the minimal value of the priming voltage in the air at normal pressure, depending on the electrode material, is about 250–0.300 V. At the same time, in the case of deposit formation from compact materials with contact breaking, the range of used voltages constitutes 15–0.200 V, which is below the minimum of Paschen's curve. Thus, the results of several researches show that at priming voltage of 100–0.200 V the size of the gap can reach the values of 5–0.10 μm [22].

According to Nemoshkalenco et al. [22], at processing by electro-erosion in the conditions when the priming voltage constitutes $U_{pr} \leq 300$ V, the gap beakdown cannot be explained on the basis of ionization avalanche for two reasons: absence of necessary voltage in the gap (for accelerating electrons which would ionize the molecules and atoms at collision) and insufficiency of a required number of collisions of electrons with molecules and atoms in the gap.

By analyzing the priming of electrical discharges due to the current of self-emission, it was noted that, in this case, it is necessary to take into account the primordial action of the electrostatic field, which can cause considerable mechanical tensions that may exceed the limit of resistance of the electrode material [24, 25]. For example, for gap breakdown voltages, the mechanical tension on the surfaces of the electrodes (calculated by the relation [25]: $\tau = \frac{E^2}{8\pi}$) constitutes about 450 MPa.

When using pulsed electrical discharges in a sub-excitation regime at surface processing, it is important to apply a pulse of small power but high voltage (12–0.24 kV) on the gap, which is responsible for the conductibility channel formation, through which the energy stored in the condenser battery of the pulse generator releases. This type of pulses is applied in the case of metal powder layer deposition [7, 37, 38]. To form deposition layers from metal powder they are introduced in the gap near the anode zone [7], in order to provide a longer duration for interaction with the plasma channel of pulsed electrical discharges.

For micrometer and millimeter sizes of the gap, it is difficult to observe and to record phenomena that are born and devolve in the gap and on electrode surfaces during PEDM. It was hypothesized that the electrode spots through which the PEDM plasma channel interact with machined surfaces are responsible for the effects that are produced on the electrode surfaces [25]. The plasma formations at
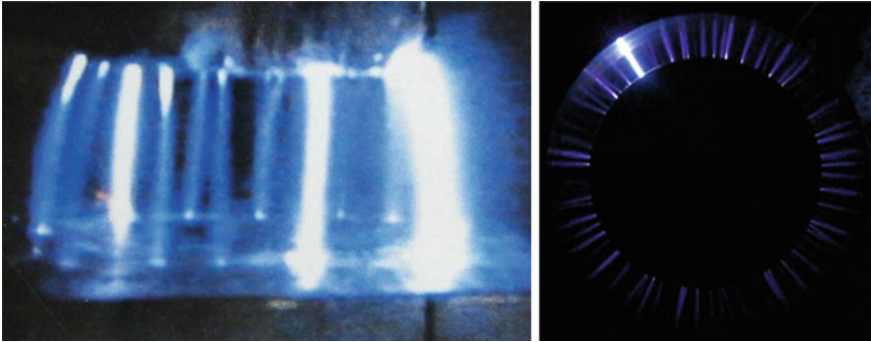
Fig. 2.1 Electrode spot and plasma channel formation at machining by applying PEDM [53]

PEDM for gaps of 10–25 mm and the charging voltage of the condenser battery of 28 kV are presented in Fig. 1 [51, 52].

From Fig. 2.1 it is clearly seen that plasma formations (of spherical shape) are born at electrodes surfaces (obvious spherical bright areas) which then develop a plasma channel mainly from the cathode to the anode. It follows that the electrode spots are responsible not only for electrical and thermal effects that occur on the electrode surfaces, but also for the effects that occur in the gap formed by their surfaces.

The supersaturated dissolution of oxygen in the construction steel was detected in the previously performed experimental research [22]. This phenomenon cannot be explained on the basis of Lazarenko's theory of interaction of electrical discharge plasma channel with electrode surfaces. The authors of several works in the field called its formation as "the condensed plasma" [40]. We propose to investigate phenomena in the gap for pulsed electrical discharges as follows: gap breakdown, emergence of the anode and cathode electrode spots, and formation of plasma channel under their action (Fig. 2.2). If such a model is accepted, the results of plasma interaction with electrode surfaces can be explained. For instance, it was suggested that electrode spots are point sources of high electric field and of heat [40]. In this case, the electric field with an intensity of 10^6–10^7 V/m arises at the cathode and anode surfaces, while the summary intensity of electric field on the gap constitutes only 10^4 V/m.

As mentioned above, the films that are formed are in amorphous state, or the amorphization process can be produced either at films' deposit from vapor or liquid state on cold surfaces or by very fine melting at depths of nanometers on the surface under the action of electrode spots. Probably, under our conditions of processing, very fine surface melting occurs at depths of nanometers of machined surface and amorphization is due to rapid cooling of the film located on the massive (in relation to the dimensions of the interaction zone) metal surface.
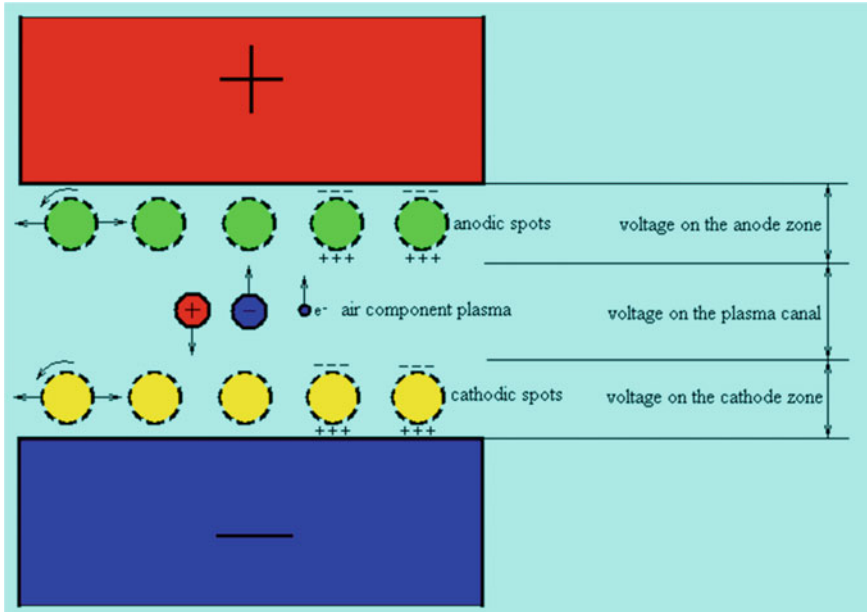
Fig. 2.2 Physical model of oxide nano-pellicle formation by applying PEDM [53]
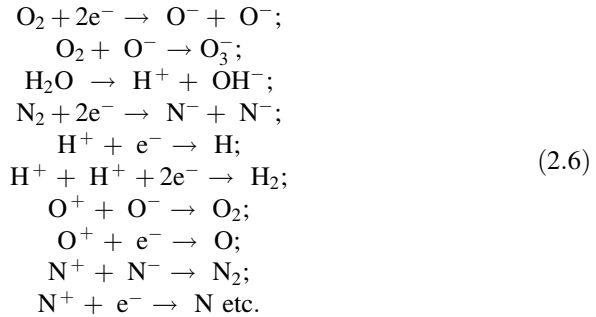
2.3   Processes of Dissociation, Ionization and Synthesis in the Plasma and on the Electrode Surfaces

In the case of using of pulsed electrical discharges under a sub-excitation regime at the surface processing, it is important to apply a low power pulseon the gap with an electric field intensity on the gap within $6–0.12 \times 10^6$ V/m, which is responsible for the formation of a conductive channel through which the energy stored in the condenser battery of the pulse generator releases. A series of phenomena are produced in the gap both at the priming phase and at the power discharge phase: electron emission, ionization, production of light radiation, thermal and sound waves, etc. We considered that the gap breakdown occurs according to Townsend mechanism and the electrons play a primordial role in all that follows.

Electrons are accelerated in the electric field of the interstice; they collide with gas molecules and atoms from the work area and produce their ionization according to the reactions [32–36, 53]:
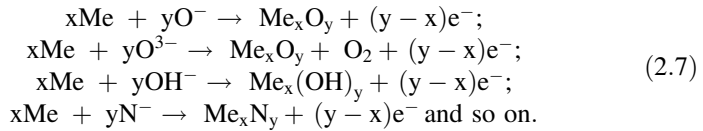
$$O_2 \rightarrow O^+ + O^+ + 2e^-;$$
$$O_2 + O^+ \rightarrow; O_3^+;$$
$$N_2 \rightarrow N^+ + N^+ + 2e^- \text{etc.} \qquad (2.5)$$
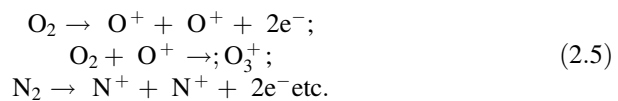
Parallel dissociation and recombination occur in the interstitial area [32–36, 53]:

$$
\begin{aligned}
O_2 + 2e^- &\rightarrow O^- + O^-; \\
O_2 + O^- &\rightarrow O_3^-; \\
H_2O &\rightarrow H^+ + OH^-; \\
N_2 + 2e^- &\rightarrow N^- + N^-; \\
H^+ + e^- &\rightarrow H; \\
H^+ + H^+ + 2e^- &\rightarrow H_2; \\
O^+ + O^- &\rightarrow O_2; \\
O^+ + e^- &\rightarrow O; \\
N^+ + N^- &\rightarrow N_2; \\
N^+ + e^- &\rightarrow N \text{ etc.}
\end{aligned}
\tag{2.6}
$$

The following chemical reactions are produced on the surface of the electrodes [32–36, 53]:

- On the anode:

$$
\begin{aligned}
xMe + yO^- &\rightarrow Me_xO_y + (y-x)e^-; \\
xMe + yO^{3-} &\rightarrow Me_xO_y + O_2 + (y-x)e^-; \\
xMe + yOH^- &\rightarrow Me_x(OH)_y + (y-x)e^-; \\
xMe + yN^- &\rightarrow Me_xN_y + (y-x)e^- \text{ and so on.}
\end{aligned}
\tag{2.7}
$$

- On the cathode:

$$
\begin{aligned}
xMe + yO^+ + (y-x)e^- &\rightarrow Me_xO_y; \\
xMe + yO^{3-} + (y-x)e^- &\rightarrow Me_xO_y + O_2; \\
xMe + yH_2O + (y-x)e^- &\rightarrow Me_x(OH)_y + \tfrac{y}{2}H_2; \\
xMe + yN^+ + (y-x)e^- &\rightarrow Me_xN_y \text{ and so on.}
\end{aligned}
\tag{2.8}
$$
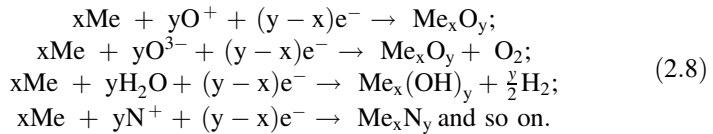
The reactions described above attest that all plasma components influence the effects occurring in the electrode surfaces, but a special role is played by the ozone synthesis process that possibly plays the most important role in the pellicle formation, being one of the chemically unstable formations of oxygen.

One can try to speculate that the process of introduction of oxygen, hydrogen and nitrogen from the air into the machined surface is similar to the magnetron cathodic sputtering system [18, 26]. However, such kinds of specullations are inadmissible for several reasons. Firstly, the electric field at PEDM constitutes 10^6–10^8 V/m, while at cathodic sputtering it is 10^3–10^5 V/m. Secondly, the gas ions at cathodic sputtering serve as energy particles to spray the target material, while in the case of PEDM they are the working agent and the medium of the surface enrichment with oxygen, hydrogen and nitrogen. It is known that in ordinary atmosphere nitrogen constitutes about 70 %, while oxygen constitutes about 27 %. In spite of this, a supersaturated dissolution of oxygen is attested.

From what has been said, we can notice that the surface oxidation occurs at the anode surface too. That is why it can function in the steady state only if its active surface is protected by one or another method, or if permanent regeneration is ensured.

2.4 Diffusion Processes at Oxide Nano-Pellicle Formation by Applyind PEDM

The determination of the diffusion coefficient and the thickness of the oxidized or hydro-oxidized surface layer also present interest in the thermal or thermochemical piece treatment by unipolar PEDM. According to the obtained results [46], and those mentioned above, we can say that, in the case of applying unipolar pulses, each cycle of thermal or thermochemical treatment develops in several steps: the step of high-temperature plasma when the discharge channel of the electrical pulse interacts with the sample surface through "cold" electrode spots with the life time of 0.2–0.0.5 μs [40]; and the low-temperature step, due to the break between the repeated action of "cold" electrode spots, as well as during the pause between two consecutive electrical discharges.

The life time of "cold" electrode spots depends on the maximum current density in the gap, and can be determined experimentally by ultrafast filming or theoretically by the relation:

$$T_{es} = \tau/N_{es}, \tag{2.9}$$

$$N_{es} = A/A_{es}, \tag{2.10}$$

where τ is the duration of the discharge pulse; N_{es} is the number of electrode spots existing during a solitary discharge; A is the area of the machined surface at a solitary electrical discharge and A_{es} is the area of the machined surface by an electrode spot.

In calculating the formed oxide film thickness we will take into account the experimental relation (2.3) obtained by Nemoskalenko [22, 29].

This paper highlights the influence of the specific energy density emitted in the gap and the properties of processed material on the process of oxide and hydroxide film formation, and can be applied for the estimation of the integral actions of plasma on the processed surface without emphasizing the real phenomena which arise in the gap and on the electrode surfaces.

Actually, the "cold" electrode spots have a migratory and selective character, as it has already been mentioned [40]. They move on the machined surface with the speed of 70–0.100 m/s and are born on its asperities and impurities. Taking into account the traces made by them on the machined surface, then for a solitary discharge, the trace made by the electrode spots is a branched one, demonstrating both their migratory nature and the fact that once the micro-oxidation takes place

the surface active resistance increases and the conditions for current flowing are aggravated. It was noticed that the character of continuity of surface processing increases when the electrical discharges were repeated. This is due to the fact that some of the asperities have been vaporized, and some impurities were subjected to volatilization. Further processing (after n cycles) demonstrates that the pellicle has a continuous character and the surface roughness constitutes Ra = 0.2–1 μm [7, 28, 29] which corresponds to the traces of "cold" electrode spots.

The processing was performed on the piece surfaces made of construction steel, titanium, aluminum and copper alloys. It was found that both the quantity of dissolved oxygen (up to 60 % at. for iron alloys, 50 % at. for copper alloys, 35 % at. for titanium alloys and 20 % at. for aluminum alloys), and its penetration depth in the sample surface differs depending on the properties of the material used. In conditions of PEDM application for surface oxidation, the most active from this point of view is the steel, followed by the alloys of Al, Ti and Cu. The above-mentioned confirms, by one or another way, the behavior of these materials in nature. If we take into account the size of atoms of each element and the compactness of crystal lattice, then the results can be described by a normal distribution [29].

The analysis of those described in the mentioned work allows one to determine the effective coefficient of elements diffusion D_{ef} by the relation:

$$D_{ef}t = N(D_1t_1 + D_2t_2 + \cdots + D_nt_n + D_it_i) \tag{2.11}$$

where N is the number of thermal or thermo-chemical treatment cycles; D_1 is the diffusion coefficient at the first interaction; D_2 is the diffusion coefficient during the interval between the two interactions with the electrode spot; D_n is the diffusion coefficient at the interaction number n; D_i is the diffusion coefficient during the interval between two consecutive interactions; t_1, t_3, ..., t_n are the durations of the interaction time of machined surface with the electrode spot during one pulsed electrical discharge; t_i is the duration of intervals between two consecutive interactions; t is the total time of thermal or thermo-chemical treatment.

Quantitatively the number of thermal or thermo-chemical treatment cycles corresponds to the number of pulsed electrical discharges on the work piece surface. Considering that each pulsed electrical discharge on the work piece surface leaves a circle shaped trace with diameter d_0, the area A_0 for which the concentration of elements is determined can be calculated by: $A_0 = \pi d_0^2/4$, If the treated surface presents a square with the side of a, then the treated surface area is $A_d = a^2$. Taking into account the fact that $A_d \geq A_0$ at the thermal or thermo chemical surface treatment by applying PEDM, it follows that the number of cycles of thermal or thermo-chemical treatment can be determined by the relation:

$$N = k(A_d/A_0)f\tau \tag{2.12}$$

where k represents the overlapping coefficient of elementary treatment zones; f is the frequency of pulsed electrical discharges; τ is the duration of thermal or thermo chemical treatment of the sample surface.

During the time interval that constitutes the pause between two consecutive electrical discharges, the redistribution of the elements in the layer deposition does not occur because the temperature is low. As a result, the speed of diffusion in this period is much smaller. It was demonstrated that the layers formed by applying PEDM are composed of two zones: the first is the substantially uniform distribution of alloying elements—called the mixing zone; and the second zone is called diffusional zone [46, 54, 55]. In the first zone complicated metallurgical processes are produced due to vaporization, melting and mixing the liquid phases of the alloying material and the matrix material part, while in the second the diffusion processes take place, caused by the thermal processes in the solid phase, at considerable depths of the work piece material. The results analyzed and presented in this chapter were obtained in the case when the machined surface was subjected to a preponderant action under the regime of diffusion of the active media elements into the work piece surface.

To describe the proposed mechanism, in accordance with previous works [46, 56–62], the one-dimensional equation of the elements diffusion from a layer of thickness h could be applied (as the original layer thickness is considered cathode strata thickness, i.e. the thickness of air between the cathodic spot and the machined workpiece surface) for a semi-infinite body:

$$\frac{\partial C_j}{\partial t} = D\frac{\partial^2 C_j}{\partial x^2}, (j = 1, \ldots, N) \tag{2.13}$$

The initial conditions for the first cycle of thermal or thermo-chemical treatment (the first interaction of the "cold" electrode spot with the machined surface) are as follows:

$$C_1(x, 0) = \begin{cases} C_0, & \text{if} \quad 0 \le x \le h; \\ 0, & \text{if} \quad x > h. \end{cases} \tag{2.14}$$

where C_0 represents the initial concentration of the piece material from the surface layer deposited on the sample's surface.

When the processed surface interacts with the "cold" electrode spots it bears a multiple character, and a portion with modified composition exists already on the surface at every consecutive interaction. For the following cycles the initial conditions are determined from the distribution of element concentration from the preceding cycle, taking into account the thickness of the formed layer:

$$C_j(x, 0) = \begin{cases} C_0, & \text{if} \quad 0 \le x \le h; \\ C_{j-1}(x - h), & \text{if} \quad x > h. \end{cases} j \ge 2. \tag{2.15}$$

According to this, the thickness h is considered constant for each cycle of thermal or thermo-chemical treatment, and it is determined separately for each case, taking into account the balance equation of the substance quantity, by the relation:

$$h = \frac{\int_0^\infty C(x)dx}{C_0 N} \qquad (2.16)$$

From this analysis, we can affirm that the effective diffusion coefficient can be determined experimentally, as described previously for the case of unipolar pulses [46]. By applying the previously described mathematical model, we can determine the formed thickness. It has been shown experimentally that the thickness of the oxide strata formed on the metal surfaces doesn't exceed micrometer order at the multiple interactions of "cold" electrode spots. In solitary interactions it doesn't exceed nanometer order.

2.5 Technology Development

As it was already mentioned [22], the effect of supersaturation of metal surfaces with atmospheric oxygen at normal pressure was detected and documented for the first time in 1990 by Nemoshkalenko et al. Then it was demonstrated that the surface oxidation with plasma is accompanied by a wide range of structural and phase modifications [22, 23, 25, 28]. Phase transformations are conditioned by the appearance of the liquid phase and deposited particle vapors that interact with the discharge channel, the surrounding environment, the cathode material and are due to the mass transfer processes in liquid and solid phase. As it was highlighted above, due to the electro-erosion processes, the cathode material can be in the "liquid-vapor" state and can interact with the environment, that's why, beside oxides, nitrides and intermetallic components, the cathode material and its other phases can usually enter the layer formed of powder [7, 29, 37, 63–69]. These conditions have been achieved in Roentgen research of the phasic superficial component for steel (steel 3, steel 45) and titanium (BT 1-0) [25, 38].

The interaction with plasma was obtained at continuous processing regime (without the inclusion of powder in the processing), when the areas of interaction were partially or multiply superposed (number of passes i was varied for the same surface portion) [25, 38]. The electrode-anode was of cylindrical form made of graphite [25, 42, 56]. The value of the gap varied between 0.15 and 2 mm, and the other parameters had the following values: the voltage on the condenser battery $U_C = 240$ V and the frequency of electrical discharges f = 40 Hz [51, 52].

The analysis of the phasic change in the composition of machined surfaces (steel 45, titanium BT 1-0) demonstrated that the basic role in these changes is not played only by the accelerated heating and cooling, but also by their interaction with the environment during processing [25, 38].

The intensity of these changes depends on the material properties and on the processing conditions, as well as on the size of the gap (which varied during the experiments, but the energy released in the gap W was constant) [25, 29].

During the processing of titanium all possible phases of its interaction with oxygen and nitrogen in the air were detected on its surface (Fig. 2.3a) [25, 29].

Oxides (TiO, TiO_2) and titanium nitride (TiN) are formed more intensively for the gap S < 1 mm. Only traces of TiO and TiN were recorded for a higher value gap (S $\approx$ 2 mm) [29]. At the multiple action of plasma, even for large values of the gap, the same phasic composition is formed on the titanium surface [29], i.e. TiO, TiO_2, TiN appear again on the surface. In this regard, the steel surfaces are less active, and the phasic composition is changed insignificantly by increasing the processing time (Fig. 2.3b) [25, 29, 38].

After the action of electrical discharge plasma on the steel surface, beside the characteristic lines of ferrite phase, the appropriate lines of austenite phase appear. The maximum amount of austenite is obtained for S $\leq$ 0.5 mm, i.e. when the attacked surface is practically covered with liquid sample material. Some of the diffractogram lines can be identified as characteristic lines of iron carbide (Fe_3C) and nitride (Fe_3N-Fe_4N) (see Fig. 2.3) [25, 29].

Fig. 2.3 Roentgenogram of superficially treated steel 45 (**a**) and titanium BT-1-0 (**b**) in the regime of "cold" electrode spots [25, 29, 38]
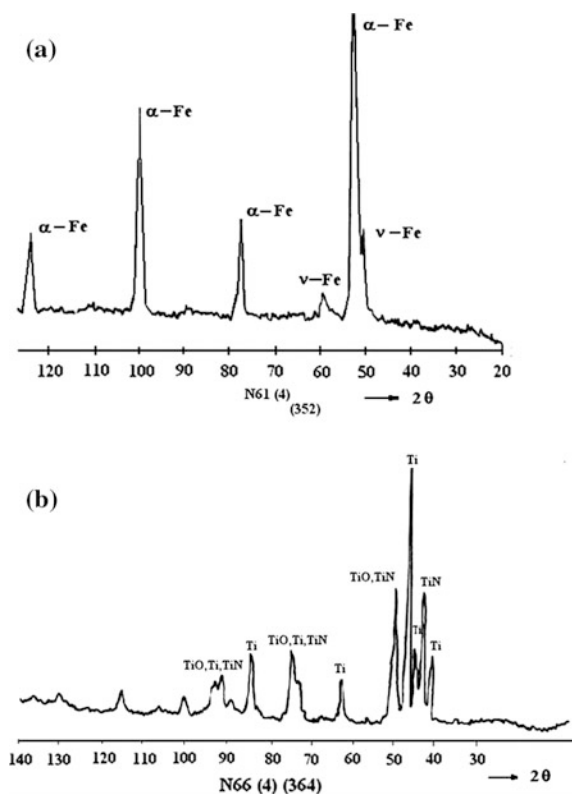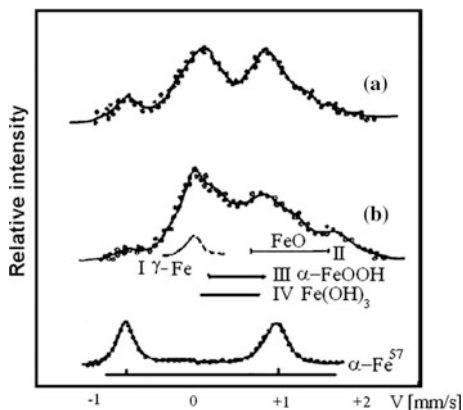
Fig. 2.4 Mössbauer spectra of steel 3 samples after machining by applying spark discharges: S = 2 mm (**a**); S = 0.5 mm (**b**) [7, 25, 29]

The presence of austenite and cementite lines in steel 3 processing is determined by the transfer through the gap of the anode material (graphite) on the cathode surface. The absence of oxides at studied regimes, according to the Roentgenogram, at the first assessment (under ordinary conditions), confirms that "colder" spots burn oxides and impurities from the surface strata [22, 25, 29], i.e. the discharge channel "migrates", in principle, on these surface defects, that, finally, leads to their removal through vaporization (this is valuable for the solitary passes). Due to this phenomenon the process of steel surface cleaning by arc-discharge in vacuum can be explained [8].

Detailed researches [23, 29] of machined surfaces by analyzing the Mossbauer spectra of steel samples (Fig. 2.4) have revealed the evidence of both spectra and represent an evasive superposition of doublets of iron oxides and hydroxides, that confirm the presence of γ-Fe phase for S = 0.5 mm. The distribution of iron, oxygen, carbon and nitrogen is shown in Fig. 2.5, a, from which it is noted that carbon is concentrated especially at the surface.

Carbon concentration decreases sharply with the increase of the surface layer depth, and the oxygen concentration reaches up to 30 % at. [25, 29]. This increased concentration of oxygen is due to the formation of hydroxides in the superficial layer of the sample. The nitrogen concentration reaches up to 5–6 % at. at layer depths up to 300 nm (Fig. 2.5) [25, 29].

For the gap of S = 2 mm, the basic components of the superficial layer are iron and oxygen, and the secondary are, respectively, carbon and nitrogen (Fig. 2.5b) [25, 29]. Oxygen concentration reaches up to 60 % at. at the surface and decreases with the increase of the sample depth. This can be explained by the fact that the hydroxides are formed at the surface and the metastable oxides are formed at depth. From the obtained roentgenograms it is seen that FeO (unique paramagnetic iron oxide at room temperature) is missing in the sample surface.

Thus, we may admit the meta-stability of some thin layers of Fe_2O_3 and Fe_3O, a fact that is well known in literature [29]. The possibility of formation of iron hydroxides in the amorphous state should not be excluded [29]. The complexity of Mossbauer
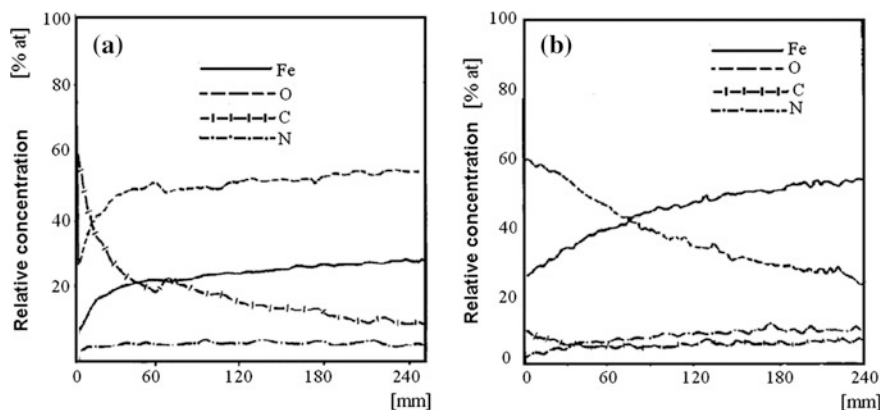
Fig. 2.5 The distribution of elements in steel 3 after PEDM for: S = 0.5 mm (**a**); S = 2 mm (**b**); *1* Fe; *2* O; *3* C; *4*—N [7, 25, 29]

spectra shows that the univocal identification of amorphous hydroxides is very difficult.

The phasic composition of titanium and steel superficial layers after removal by rectification of a layer whose thickness is 5–0.10 μm changes insignificantly: the amount of oxides decreases on the titanium surface while that of nitrides decreases on the steel surface. The change of the energy regime does not cause significant qualitative changes, only quantitative changes occur (for S = *const*) [25, 29].

Thus, the study of diffractograms has shown that the most important technological parameters which influence the phase composition of the surface are the value of the gap and the duration of the interaction with the plasma (the number of passes), respectively.

Recently, a number of works [32–36, 42–46, 53–56] have been published, where the results on electro-discharge oxidation of metal surfaces under ordinary conditions are presented. Coatings obtained by this method usually have a dual structure. It consists of an inner base layer at the edge of the metal-coating and an external outer layer.

The base layer is fine-porous, has a crystalline structure and constitutes 60–90 % of the coating thickness. The outer layer coating is less hard, more porous, has an amorphous state and takes on 40–10 % of the thickness.

The coating under the oxidation process is able to germinate in metals in about 10–60 % of the total thickness of the coating in depth and consists mainly of oxides of the elements contained in the machined alloy and elements from the interstice.

The PEDM method allows to form coatings on pieces of complex shapes and of any configuration [70], including the internal surface of pipes [35].

In order to develop the technology of oxide film formation, the duration and the form of the pulse, the energy and the power released in the gap at a singular discharge, the size of the gap and the frequency of pulses were chosen as input

parameters of the technological process, and the thickness of the oxide films, the width of oxidation strips, the productivity of the technological process, the micro hardness of the processed surface layer, the surface electrical resistance, and the corrosion resistance were chosen as output parameters.

To perform the experimental research aiming at the appreciation of the oxidation strip width depending on the sample material and the processing energy regime we used the current pulse generator with priming from a block of high voltage of 12 kV and of 0.3 µA current [29], the laboratory setup that ensures the positioning, fixing and rotating of the samples in the process of machining with the rotation frequency adjustable within 0 and 150 rot/min.

The used tool-electrode was made in the form of cylindrical bar rounded at the working end of the hemispheric shape and made of the same material as the work piece to avoid the appearance of foreign phases in the machined surface as a result of electrical erosion. The cathode work piece presents a cylinder of Ø11.28 mm. The anode tool-electrode is a Ø6 mm cylinder with a semicircular end.

The generator for the formation of oxide films on metal piece surfaces by applying PEDM contains the following blocks: the power pulse generator, the priming block (intended to initiate electrical discharges) and the control block whose role is to synchronize the power and priming pulses [29, 45, 53].

The pulse current generator [29, 45, 53] with a voltage block for interstice pre-ionization was used as a source of energy. The discharge energy emitted in the interstice constitutes 1–6 J. Thus, by establishing the generator energy regime, the superficial piece oxidation for indicated materials without melting the processed surface can be produced. The superficial piece oxidation for indicated materials without melting the processed surface can be produced to establish the generator energy regime.

The thickness of the oxide pellicle subjected to the condition of the energy balance and according to Palatnik's criterion [29, 45, 53] is directly proportional, respectively, to the quantity of heat and the energy emitted on the electrode surfaces:

$$
\begin{aligned}
\delta &\sim Q; \\
\delta &\sim W_s.
\end{aligned}
\qquad (2.17)
$$

The power of electrical discharge:

$$
P = \frac{dW_s}{dt} = \frac{W_s}{\tau} \qquad (2.18)
$$

where τ is the duration of electrical discharge.

From the other point of view, the thickness of the oxide pellicle depends on the physical properties of the processed surface material [29]:

$$\delta \sim \sqrt{\rho \cdot c \cdot \lambda},\qquad\qquad(2.19)$$

where ρ is material density; c is specific thermal conductibility; λ is specific melting heat.

Thus the thickness of the oxide pellicle is directly proportional to the power of electrical discharge emitted in the interstice and depends on the physical properties of the processed surface material.

The technological schemes used in the formation of the oxide pellicles by applying PEDM are shown in Fig. 2.6. The work-piece was connected in the discharge circuit as a cathode, and the tool-electrode—as an anode.

The direct determination of operating properties that affect the functionality of pieces has required intensive investigations. Therefore, this task has been addressed in a manner that does no require the use of lengthy and expensive techniques and equipment.

Following the analysis of literature [29, 45, 53] we concluded that the RC type generators with parallel priming can be successfully used for micro- and nano-oxidation of the conductive piece surface. The measurement of the oxidation strip size was performed in a continuous processing regime at solitary zones of plasma channel interaction with surface samples with overlap coefficient $k_{sp} = 0.5$, and the rotational frequency was established according to the frequency of PEDM taking into account the value of k_{sp}. The width of the strips was appreciated for various materials and processing technological regimes.

The strip width of the oxide films was measured with a microscope of the type METAM with measurement accuracy of ±0.025 mm.

Because the oxide films have small thickness, the current exceeding mA should not pass through them. Therefor, it is necessary to measure the resistance with the use of a bridge that should divide the current from the ohmmeter source. The oxide film having high electrical resistance R_p (of the order of MΩ) is shunted by a much smaller ohmic resistance, R_{sh} (of the order of tens of kΩ), and then the maximum of the total current should pass through the shunt resistor.
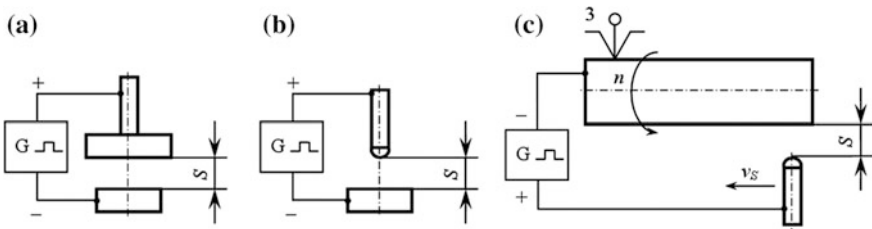

Fig. 2.6 The technological schemes of the oxide pellicle formation by applying PED: **a** on the plane surface with plane tool-electrode; **b** on the plane surface with a semi circular tool-electrode; **c** on the exterior cylindrical surfaces [53]

The measurement of electrical resistance of samples before processing is done using a digital ohmmeter with a measurement limit of tenths or hundredths of Ω, because the metallic samples are good electrical conductors.

Electrolytes made of chemical agents dissolved in distilled water at room temperature having a certain concentration were prepared to perform investigations on resistance to chemical corrosion of processed samples (with oxide films formed on the active surface by applying PEDM). The oxide films were formed by applying PEDM with optimal energy parameters for each investigated material.

The samples were fixed in the developed device so that only a circular portion of the machined surface was subjected to dissolution. It was included in the circuit of anodic dissolution as anode. The investigations were performed in DC regime with step-by-step changing of the applied voltage of 0.1 V.

The speed of corrosion is determined by weighing the samples before and after the investigations using the analytical balance of type VL-200 with an accuracy of 10^{-4} g.

The index of the corrosion speed is determined by the relation [53]:

$$K = \frac{\Delta m}{S \cdot t};$$
(2.20)

where K is the speed of corrosion (the mass index), g/m^2·h; S is the area of the work piece surface, m^2; t is the duration of investigation (working time), h; Δm is the loss (or the addition) in the work piece mass, g;

$$\Delta m = m_i - m_f;$$
(2.21)

where m_i is the initial mass of the sample, g; m_f is the final mass of the sample, g.

The conditions under which the investigations were performed for experimental determination of corrosion speed are as follows: the sample—anode; the voltage between the electrodes U = 2 V; the distance between the electrodes d = 10 mm; the electrolyte is composed of aqueous solution of 3 % NaCl at room temperature for samples made of construction steel, or of 30 % H_2SO_4 at the temperature of 80 °C for titanium alloy samples; the processing time at each measuring step t = 0.5 h; the work piece surface area (the area of contact with the electrolyte) S = 50.24 mm^2.

2.6 Results of Experimental Investigations and Their Analysis

2.6.1 Results of Technological Investigations on Film Formation

Next we will present the results of experimental research on the formation of oxide films on metal surfaces by applying PEDM. It has been experimentally established

that the surface oxidation is more effective when the work piece is connected in the discharge circuit as cathode (direct polarity). Below are presented the dependencies of the output parameters upon the input ones with their approximation by mathematical modeling. The productivity of oxide films formation is optimized. The next results show the interdependence between the chemical and phase composition of the formed films and their properties. It was found that the micro hardness of the processed surface layer increases by 30–100 HV units, the surface electrical resistance increases by about 10^7 times, the corrosion speed decreases by at least 2 times for construction steels and by 100 times—for titanium alloys compared with the unprocessed surface.

The dependence of oxide layer thickness δ on the power dissipated in the gap at a solitary discharge is shown in Fig. 2.7, while its dependence on the gap size is presented in Fig. 2.8.

Fig. 2.7 The dependence of the oxide film thickness on the power dissipated in the gap [53]. The work piece-cathode and the tool-electrode material: ♦—titanium alloy BT8; ■—steel 45; ▲—BrA5 copper alloy; ●—aluminum alloy D16. The processing scheme according to Fig. 2.6a
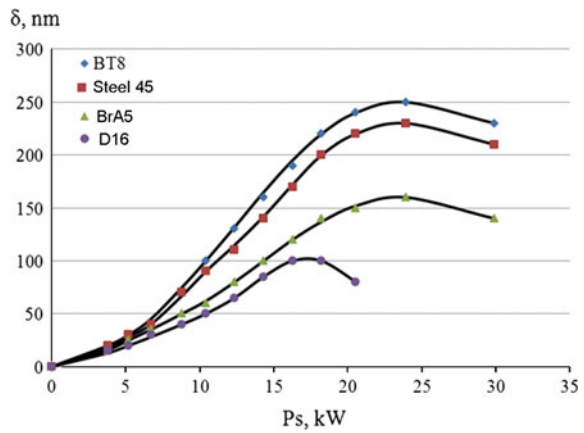
Fig. 2.8 The dependence of the oxide film thickness on the gap size [53]. The work piece-cathode and the tool-electrode material: ♦—titanium alloy BT8; ■—steel 45; ▲—BrA5 copper alloy; ●—aluminum alloy D16. The processing scheme according to Fig. 2.6a
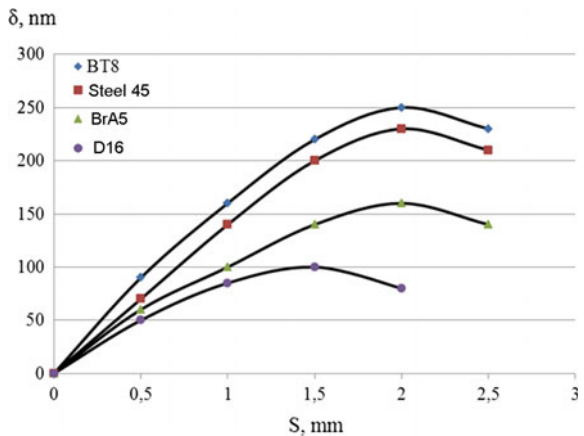
By analyzing the curves shown in Figs. 2.7 and 2.8 we can see that the thickness of the oxide strata increases exponentially with the value of input energy parameters regardless of the physico-mechanical properties of the piece material. This can be explained by the fact that the efficiency of the energy and, respectively, the power dissipated in the gap becomes higher with the increase of their values. At the same time, the increase of the gap active resistance is attesting and the greater amount of energy is spent on such secondary effects as brightness and sound intensity increase created by the shock wave.

When applying the pulsed electrical discharge power greater than that of critical value (for titanium, iron and copper alloys this value is 30 kW and for aluminum alloys it is 20 kW) the intensity of evaporation of the work piece surface layer enhances, which leads to the decrease of the oxide film thickness.

The optimum value of the pulse power for the surface oxidation of the metal surface is $P_S = 20{-}0.30$ kW at the gap sizes of $S = 1.5{-}0.2$ mm for iron, titanium and copper alloys, and $P_S = 15{-}0.20$ kW at $S = 1.0{-}1.5$ mm for aluminum alloys, respectively.

The experimental research results on the determination of oxidizing strip width dependence on the energy processing regime are shown in Fig. 2.9.

Referring to Fig. 2.9 we can see that the dependencies of the processed strip width on the work piece-cathode surface upon the power dissipated in the gap represents an exponential dependence for all processed materials. The process is conducted more intensively on the sample surfaces made of titanium alloy, than on those made of steel, copper alloy, and the last one is the aluminum alloy. These effects can be explained on the basis of thermo-physical properties, of electron emission for these materials, and of the avidity of their constituent elements to oxygen.

Technological dependencies obtained after mathematical processing according to the described methodology [36, 45, 53, 54] can be approximated by the equations:

Fig. 2.9 Dependence of the oxidizing strip width on the pulse power dissipated in the gap [53] for samples made of: ♦—D16; ■—steel45; ▲—BT8. The processing scheme according to Fig. 2.6c
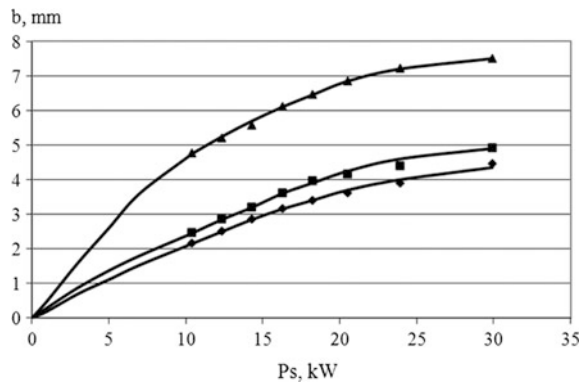
(1) The film thickness on the gap size:

$$\delta_{Ti} = \frac{373 \cdot S^{1.53}}{e^{0.77 \cdot S}} \, ; \, \delta_{Fe} = \frac{379 \cdot S^{1.82}}{e^{0.91 \cdot S}} \, ; \, \delta_{Cu} = \frac{231 \cdot S^{1.46}}{e^{0.73 \cdot S}} \, ; \, \delta_{Al} = \frac{213 \cdot S^{1.51}}{e^{1.01 \cdot S}} \, ;$$

(2.22)

(2) The film thickness on the power dissipated in the interstice:

$$\delta_{Ti} = \frac{0.12 \cdot P_S^{3.52}}{e^{0.15 \cdot P_S}} \, ; \, \delta_{Fe} = \frac{0.08 \cdot P_S^{3,67}}{e^{0.15 \cdot P_S}} \, ; \, \delta_{Cu} = \frac{0.05 \cdot P_S^{3.66}}{e^{0.15 \cdot P_S}} \, ; \, \delta_{Al} = \frac{0.01 \cdot P_S^{5,08}}{e^{0.28 \cdot P_S}} \, .$$

(2.23)

(3) The oxide film strip on the power dissipated in the interstice:

$$b_{Al} = 0.46 \cdot P_S^{0.68} ; b_{Fe} = 0.55 \cdot P_S^{0.66} ; b_{Ti} = 1.66 \cdot P_S^{0.46} .$$

(2.24)

For quantitative assessment of productivity, the specific processing time T (s/cm^2) or (min/cm^2) was measured, which presents the processing time of a surface with the area A = 1 cm^2. As it has already been mentioned the electrode spots are migratory and they scan the machined surface depending on the impurities presented on it or on its roughness "seeking" the place with the lowest electrical resistance of the gap. The electrode spot can randomly migrate on the surface, but by adjusting or setting the priming voltage pulse we can organize desired surface machining without breaking the formed film. Figure 2.10 shows the photos of unprocessed surface and of the work piece surface consecutively processed by one and several solitary discharges.

The technological scheme applied to such processing corresponds to Fig. 2.6a, i.e. electrical discharges occur between two flat parallel surfaces. The traces of plasma channel interaction with the machined surface confirm the migratory character of the electrode spots and the hypothesis that the electrical discharges occur in the gap zones with the lowest active resistance.

In the case when the tool-electrode dimensions and the geometric shape are different from those of the machined surface the situation changes in the gap, and the electric discharge can only develop along the radius vector of the electric field that corresponds to the intensity necessary for dielectric environment breakdown. It follows that by setting a certain value of priming voltage applied to the gap and its certain size we can manage the sequence of plasma (electrode spots) interactions with the machined surface, and, thus, we can elaborate the nano-oxidation technology of surfaces with a large area and a complicated geometry. Figure 2.11 can serve as an example.

Thus, by applying PEDM, we can process conjugated surfaces of different shapes (e.g. flat surface with flat tool-electrode) with the formation of continuous oxide films, or we can form discrete oxide stripes using a rounded bar tool-electrode. The oxidation strip width will depend on the tool-electrode geometry and processing energy regime.
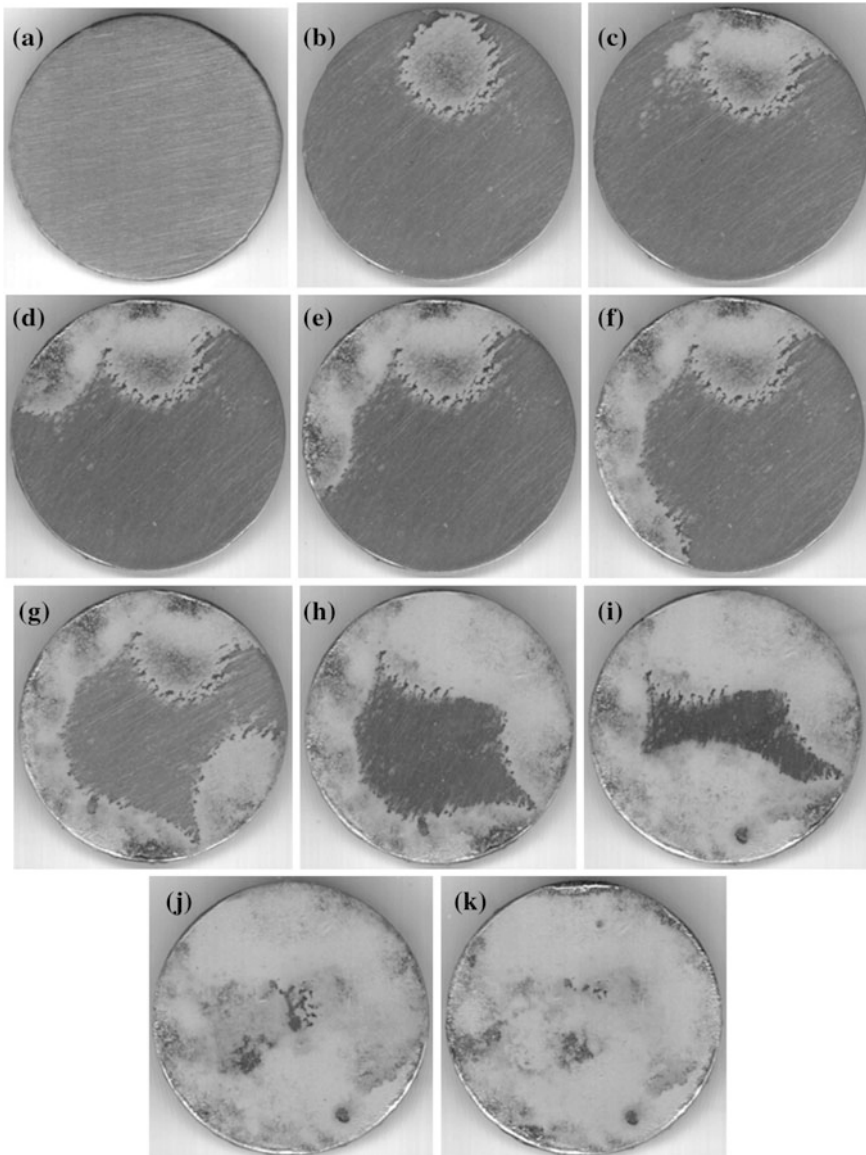
Fig. 2.10 A general view of unprocessed and processed flat surface by applying PEDM with flat tool-electrode, × 4 [53]. Energetic processing regime: the size of the gap S = 2 mm; charging voltage of the condenser battery U_C = 240 V; its capacity C = 600 μF; the energy released in the gap W_S = 5.27 J; the duration of the power pulse τ = 220 mS. The number of solitary pulses, *i*: **a** 0 (unprocessed surface); **b** 1; **c** 2; **d** 3; **e** 4; **f** 5; **g** 10; **h** 15; **i** 20; **j** 25; **k** 30. Work piece and tool-electrode material—titanium alloy BT-8
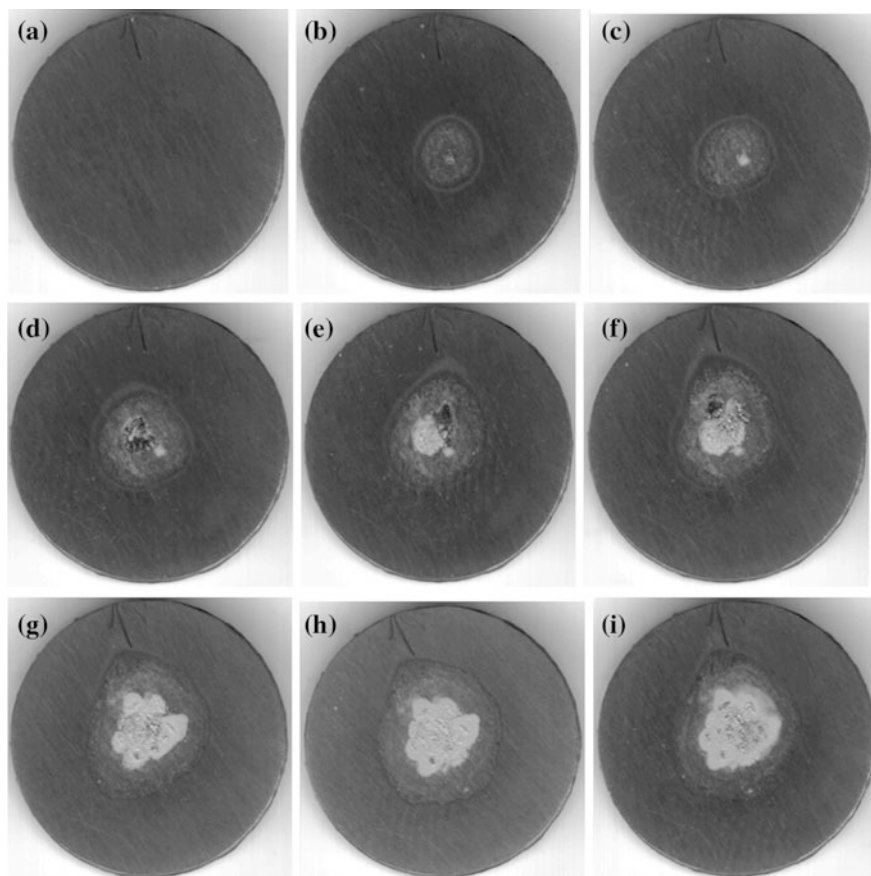
Fig. 2.11 A general view of unprocessed and processed flat surface by applying PEDM with semi-circular (Ø6 mm bar) tool-electrode, × 4 [53]. Energetic processing regime: the size of the gap S = 1.5 mm; charging voltage of the condenser battery U_C = 140 V; its capacity C = 600 μF; the energy released in the gap W_S = 3.15 J; the duration of the power pulse τ = 220 mS. The number of solitary pulses, *i*: **a** 0 (unprocessed surface); **b** 1; **c** 2; **d** 3; **e** 4; **f** 5; **g** 10; **h** 15; **i** 20. Work piece and tool-electrode material—titanium alloy BT-8

The end of processing is recorded at the time when no discharge occurs between the examined samples, which indicates that a continuous oxide film is formed on the surface with the active surface resistance that exceeds the initial parameters of the processing regime.

The productivity is calculated as the inverse value of the specific processing time [53, 58]:

$$\eta = \frac{1}{T} \ (cm^2/min).\tag{2.25}$$

The research results of the dependence of the film formation productivity on the input parameters (the pulse frequency, the energy released in the gap, and the size of the gap) are presented in Figs. 2.12, 2.13 and 2.14.

With the increase of the pulse discharge frequency (from 0 to 15 Hz) the productivity increases, reaching the maximum value $\eta \approx 2.14$ cm^2/min for f = 15 Hz. For the values f > 15 Hz the productivity decreases hyperbolically (Fig. 2.12).

The decrease of productivity of oxide films formation is due to the fact that the condenser battery does not succeed in loading totally, and the work environment from the gap does not restore completely. Therefore, the energy discharge decreases, which leads to the constriction of the plasma channel, and, as a result, to the decrease of the chemico-thermal influence of the zone of the work piece surface. To annihilate the undesirable effect, we propose to decrease the value of the ballast resistance (or the ballast resistance is to be replaced by an electronic key) in

Fig. 2.12 Dependence of the specific processing time (♦) and of the productivity of oxide films formation (■) for steel 45 mating surfaces of the electrodes on the pulse frequency: the gap size S = 2 mm; the capacity of the condenser battery C = 600 μF; the charging voltage of the condenser battery Uc = 240 V. Processing scheme according to Fig. 2.6a [53]
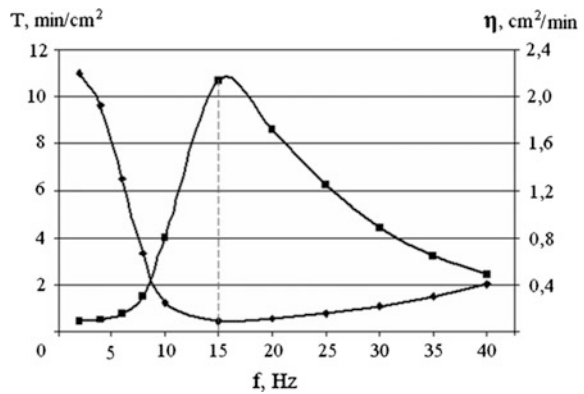

Fig. 2.13 Dependence of the specific processing time (♦) and of the productivity of oxide films formation (▲) for steel 45 mating surfaces of the electrodes on the energy released in the gap: The pulse frequency f = 15 Hz. Processing scheme according to Fig. 2.6a [53]
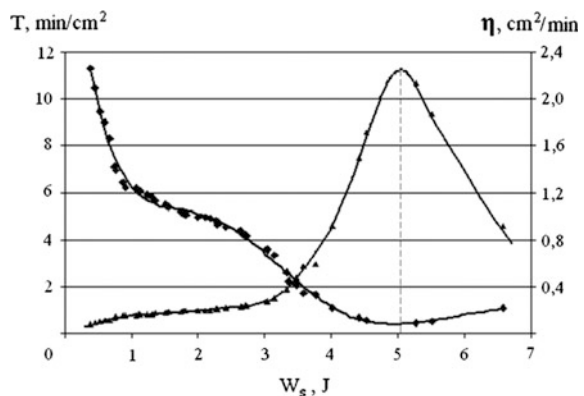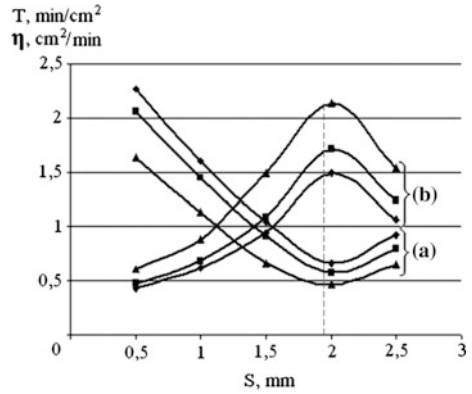
Fig. 2.14 Dependence of the specific processing time (♦) and of the productivity of oxide films formation (▲) for steel 45 mating surfaces of electrodes on the gap size: the energy released in the gap Ws: ♦—3.5–4 J; ▲—4–4.5 J; ■—4.5–5 J; the capacity of the condenser battery C = 600 μF; the pulse frequency f = 15 Hz. Processing scheme according to Fig. 2.6a [53]

order to decrease the loading time of the condenser battery of the pulse generator, to provide additional oxygen supply for the gap, and to restore the interstitial environment. Considering the optimal value of the pulse frequency, for which the maximum of productivity is obtained, the further researches on the influence of other parameters on the productivity of oxide films formation were made for f = 15 Hz.

The observed maximum in the dependence of the productivity of oxide film formation on the energy released in the gap (Fig. 2.13) (for $W_S \approx 5$ J, the capacity of the capacitor C = 600 μF, the charging voltage of the condenser battery U_C = 240 V, and the gap size S = 2 mm) can be explained by the fact that at higher energies released on the surface layer of the sample, beside the "cold" electrode spots, "hot" electrode spots are functioning, causing material melting and vaporization of the machined surface (together with the film rich in oxides) in the interaction zone with the plasma channel, which leads to its renewal and, therefore, to the possibility of gap breakdown.

As it was previously established [29], the dependence of the volume of the hot central zone of the plasma channel upon the size of the gap gets a maximum for S = 1.5–2 mm when the energy released in the gap is W_S = 3.5–6 J. The maximum of heat quantity in the plasma channel corresponds to the maximum of productivity from Fig. 2.14 (for all 3 cases (Ws = 3.5–4 J, Ws = 4–4.5 J and Ws = 4.5–5 J) the maximum was obtained for S = 1.5–2 mm).

Thus, taking into account the influence of PEDM parameters on the intensity of oxide film formation on the conjugated surfaces of pieces made of structural steel, the optimal processing regime was set: the pulse frequency f = 15 Hz; the gap size S = 1.5–2 mm; the capacity of the condenser battery of the power generator C = 600 μF; the charging voltage of the condenser battery U_c = 240 V (the average value of the energy released in the gap for these values Ws = 5.27 J). The specific processing time in this case does not exceed 0.5 min/cm^2 and the productivity is $\eta \approx 2.14$ cm^2/min.

2.6.2   Phase Composition of Nano-Oxide Films

An example of high-resolution XPS oxygen spectrum is shown by curve 1 in Fig. 2.15. The spectra were obtained using XPS and PHI SUMMIT processing—by using PHI Multipack 8.2 C. The standard procedure is described in details elsewhere [46], based on the characteristics of the Versa Probe 5000 equipment.

The signal analysis revealed the presence of oxygen O−1 s in three types of chemical bonds (called components). These are as follows: (a) the component O^{-2} (which contains oxygen atoms of metal oxides, in the sample labeled number 3 in Fig. 2.15), with the specific energy 529.6 EV; (b) the component of OH− with EV 531.5 (indicated by the numeral 2 in Fig. 2.15c) the component of type O–C and O–C=O with EV 533.4 (indicated by 4 in Fig. 2.15).

The chemical analysis showed the concentration of each of the three components (C) (a): (C) (b): C (c) = 0.89: 1.00: 0.50. Additional studies have shown a possible existence of a fourth component of oxygen within the context of type O-H_2. However, the relative concentration of this component value is assumed to be not greater than 0.15.

Studies have proven that virtually there is no change in the geometry of the original surface when applying the PEDM method for the formation of oxide coatings. This makes it possible to recommend this method for surface processing of completed parts. The thickness of films is between 10–240 nm [32, 35, 53], i.e. it corresponds to the field of nanotechnology.

The abnormal dissolution of oxygen in metals is observed when processing metal surfaces by this method [53]. For instance, when processing samples made of structural steel, the dissolution of oxygen reaches 59 % at., while this value is around 34, 19, and 39 % at. for samples made of titanium alloys, aluminum alloys, and copper alloys, respecively.

Fig. 2.15 XPS spectrum of oxygen of oxide pellicles on samples of steel 45: *1* total spectrum; *2* OH− component; *3* O^{2-} component; *4* components of O–C and O C=O types
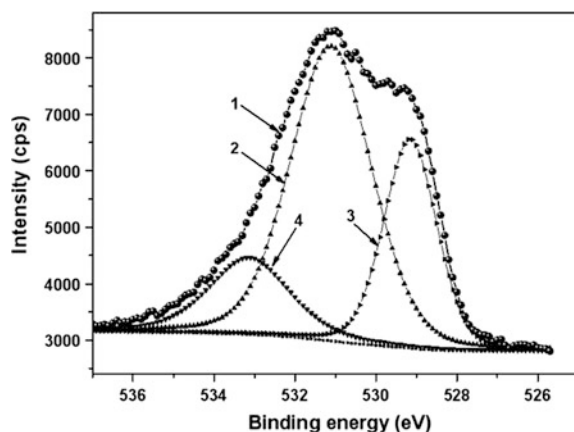
The metal oxides in the pellicle are in amorphous state. This probably explains why the surface resistance for steel pieces increases up to 10^6 Ω/mm^2 [32, 53], the potential to corrosion increases by 10 or more times, and the corrosion speed is reduced by 2–0.4 times [32, 34, 53].

2.6.3 Morphology and Chemical Composition of Nano-Oxide Films

The results of SEM and EDX analysis of investigated sample surfaces are presented in Figs. 2.16, 2.17, 2.18, 2.19, 2.20 and 2.21 and in Table 2.1.

As we can see from these results, the abnormal dissolution of oxygen in metals is observed while processing metal surfaces by this method [22, 53, 56, 59]. It is
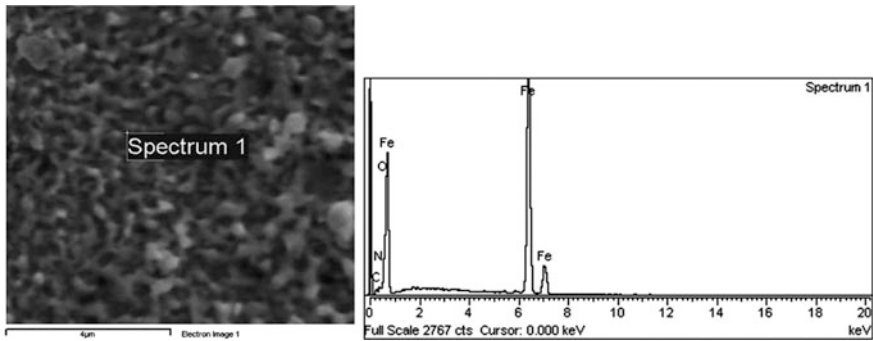

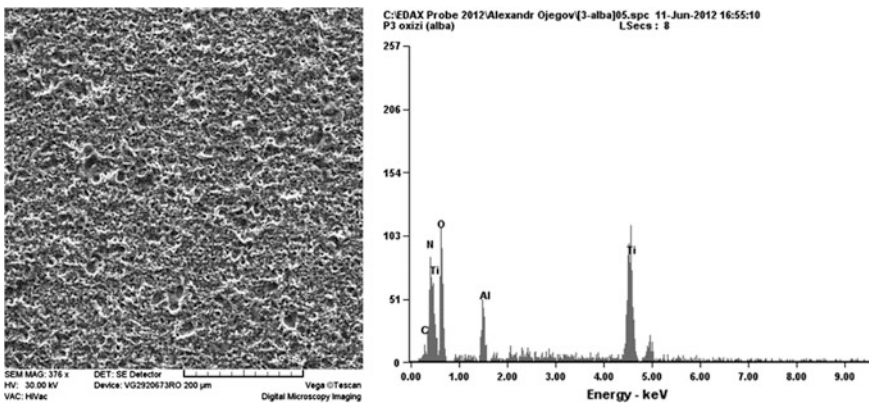**Fig. 2.16** SEM and EDX analysis of steel 45 sample surface [53]

Fig. 2.17 SEM and EDX analysis of BT8 titanium alloy sample surface [53]
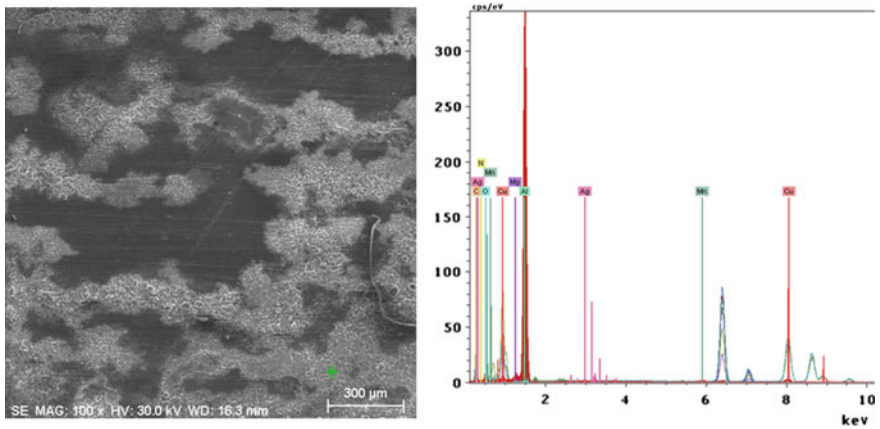
Fig. 2.18 SEM and EDX analysis of D16 aluminum alloy sample surface [53]
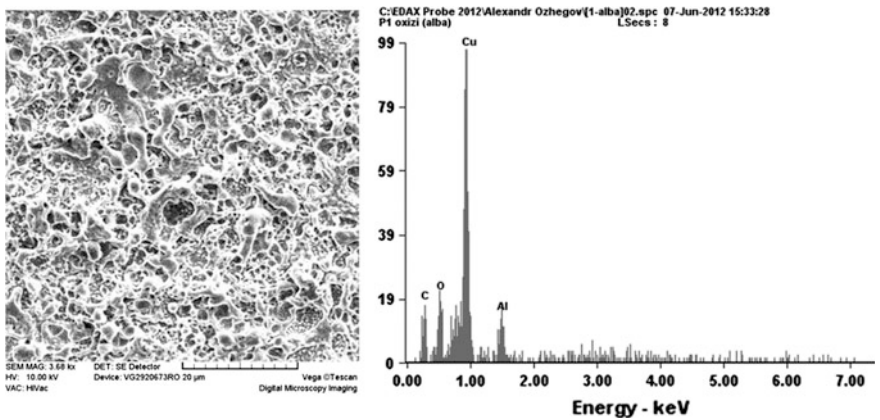

Fig. 2.19 SEM and EDX analysis of M0 copper alloy sample surface [53]

demonstrated that the dissolution of oxygen when processing the samples made of construction steel reaches 60 % at., while this value is around 30–35, 20, and 50 % at. for samples made of titanium alloys, aluminum alloys, and copper alloys, respectively. The superficial layer of steel and titanium alloy surfaces contains nitrogen, besides oxygen.

Still in one of the first works dedicated to the surface processing by applying PEDM in the regime of its maintenance on the "cold" electrode spots [29] it was demonstrated that the reduction of the initial surface roughness is attested in all the cases. If we analyze the images shown in Fig. 2.22b, hich represents the morphology of the processed surface layer, we find that the quality of the surface with the oxide film (Ra ≈ 0.1–0.2 μm) is increased as compared to the mechanically machined surface (Ra ≈ 0.63 μm, Fig. 2.22a). This phenomenon can be explained
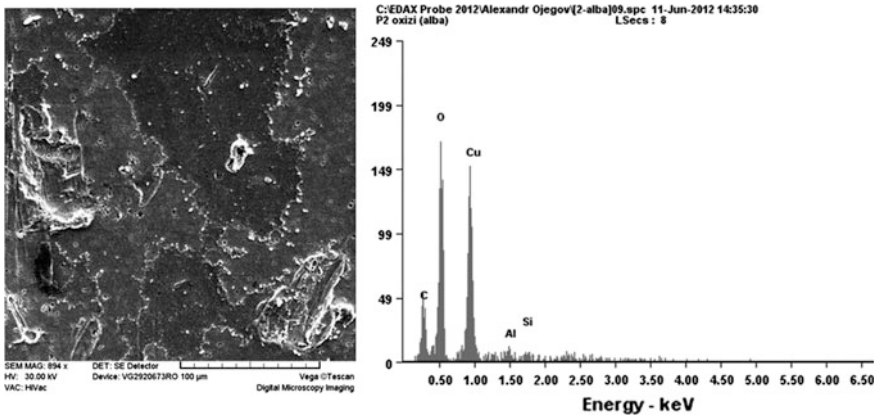
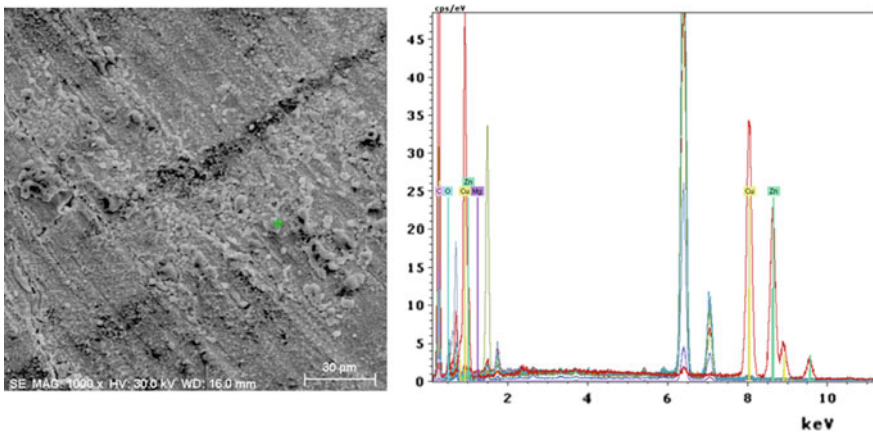**Fig. 2.20** SEM and EDX analysis of brass L63 sample surface [53]

Fig. 2.21 SEM and EDX analysis of bronze BrA5 sample surface [53]

by the fact that the asperities formed on the surface of the sample as a result of mechanical machining are subjected to vaporization and electrical erosion in the solid, liquid and vapor state under the action of strong electric fields and of PEDM plasma.

2.6.4 Surface Electrical Resistance

The results of investigations of surfaces subjected to the oxidation process under the maintenance of PEDM by "cold" electrode spots are presented in Fig. 2.23. It is seen that for the cathode–work piece (Fig. 2.23a) the processing has taken place

Table 2.1 The EDX analysis of sample element content [53]

Basis material of the sample	EDX element content of processed surface		
	Element	(norm. wt%)	(norm. at.%)
Steel 45 (C45)	Carbon	1.89	4.32
	Nitrogen	7.82	12.43
	Oxygen	29.77	58.74
	Iron	60.52	24.51
Titanium alloy BT8 (TiAl6Mo4)	Carbon	00.41	01.38
	Oxygen	30.33	33.27
	Nitrogen	03.38	09.56
	Aluminum	05.84	08.57
	Titanium	60.04	47.22
Aluminum alloy D16 (AlCu4Mg1)	Aluminum	66.84	55.68
	Oxygen	13.95	19.60
	Magnesium	2.49	2.30
	Carbon	1.82	3.40
	Copper	2.42	0.86
	Manganese	0.55	0.23
	Silver	0.86	0.18
Technically pure copper M0	Copper	59.5	25.55
	Oxygen	29.53	50.50
	Carbon	10.22	23.20
	Aluminum	0.75	0.76
Bronze BrA5 (Cu95Al5)	Copper	52.97	21.18
	Oxygen	26.66	42.34
	Carbon	14.83	31.38
	Aluminum	02.66	02.50
	Silicate	02.87	02.60
Brass L63 (Cu63Zn37)	Copper	42.30	23.25
	Zinc	32.89	17.57
	Oxygen	16.72	36.50
	Carbon	7.52	21.86
	Magnesium	0.57	0.82

over the entire surface, while on the anode-surface sample (Fig. 2.23b) traces of plasma channel migration are clearly observed (areas with more light color), and among these areas darker color areas are observed (where the electrode surface interacts with the peripheral plasma channel).

For the first time, the surface electrical resistance was measured in the samples made of steel 45 processed by applying PEDM (Table 2.2) both for the anode-tool-electrode and for the cathode-work piece surfaces. The surface electrical resistance of the unprocessed samples is comprised within the limits of 0.05–0.09 Ω/mm^2. By analyzing the results presented in Table 2.2 we can attest a substantial
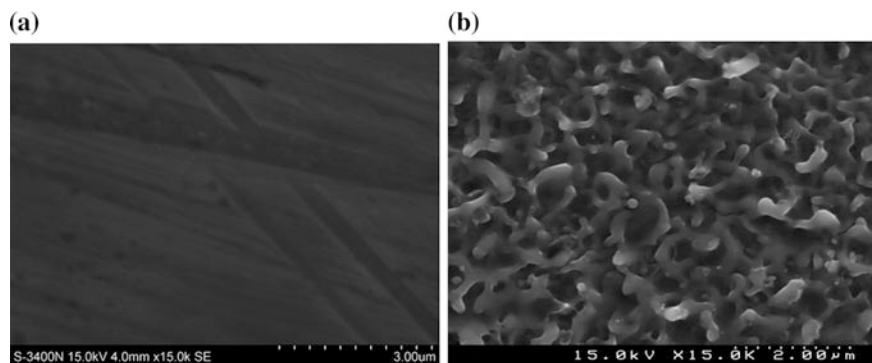
Fig. 2.22 Morphology of the superficial strata of the work pieces: **a** unprocessed surface; **b** surface processed by applying [53]
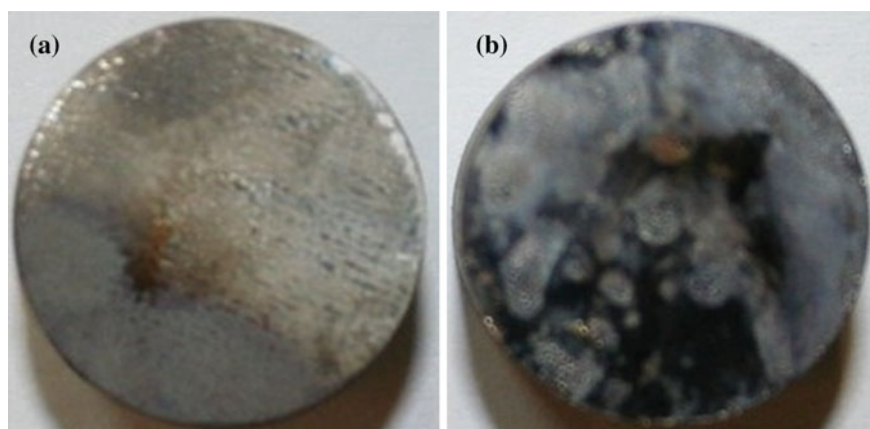

Fig. 2.23 General view of the samples made of steel 45 processed by applying PEDM (the capacity of the condenser battery C = 600 μF, the charging voltage of the condenser battery U_c = 160 V, the distance between electrodes (the gap size) S = 1.5 mm, the pulse frequency f = 15 Hz, the energy accumulated on the condenser battery W_C = 7.68 J, the energy released in the gap W_S = 3.58 J): **a** sample—cathode; **b** sample—anode [53]

increase of the surface electrical resistance of the electrodes that have participated in the PEDM process in all cases. However, the active surface resistance of the anode-electrode is about 3 times lower than that of the cathode. This latter finding can be explained by the fact that, under the same conditions, a larger amount of energy is released on the anode surface, and it is possible that more intense vaporization process occurs. That is why the oxide film formation is slower.

Next, the surface electrical resistance of the surerficial stratum for cathode-samples made of titanium, aluminum and copper alloys was measured (Table 2.3).

Table 2.2 Surface electrical resistance of oxide pellicles on samples of steel 45 [53]

Sample	Surface electrical resistance ($\times 10^6$ Ω/mm^2)				
	Experimental data				Average value
Cathode	0.88	0.72	1.46	0.71	0.98
	0.97	1.52	0.68	0.72	
	0.73	1.09	0.76	0.83	
	1.33	1.10	1.04	0.73	
	1.07	0.88	1.21	0.78	
Anode	0.81	0.26	0.46	0.31	0.33
	0.11	0.14	0.56	0.34	
	0.29	0.11	0.62	0.38	
	0.87	0.38	0.11	0.15	
	0.12	0.13	0.27	0.17	

Table 2.3 Surface electrical resistance of the oxide pellicles formed on the surfaces of cathode—samples [53]

Base material of the processed samples	Average value of the surface electrical resistance ($\times 10^6$ Ω/mm^2)
Titanium alloy BT8	1.6
Duralumin D16	0.25
Technically pure copper M0	0.15
Bronze BrA5	0.17
Brass L63	0.19

As one can see from the results presented in Tables 2.2 and 2.3, the surface electrical resistance depends on the investigated sample material, and it has higher values for materials with lower electrical conductivity.

2.6.5 Resistance to Corrosion

The sufficient and necessary conditions were established for avoiding the appearance of the liquid phase on the surface of processed samples [32–36, 42–46, 53–56]. Avoiding the emergence of a liquid phase is necessary for two reasons: to omit the erosion process of the processed surface and the crater formation, and, as a result, to avoid the increase of the final processed surface roughness.

The microscopic surface investigation of two identical samples made of steel 45 (Fig. 2.24a—the surface with oxide films, Fig. 2.24b—the unprocessed surface) after 3 years of their storage in air in ordinary conditions shows that rust appeared on the unprocessed surface. As for the machined surface, no interaction with the environment was noticed.
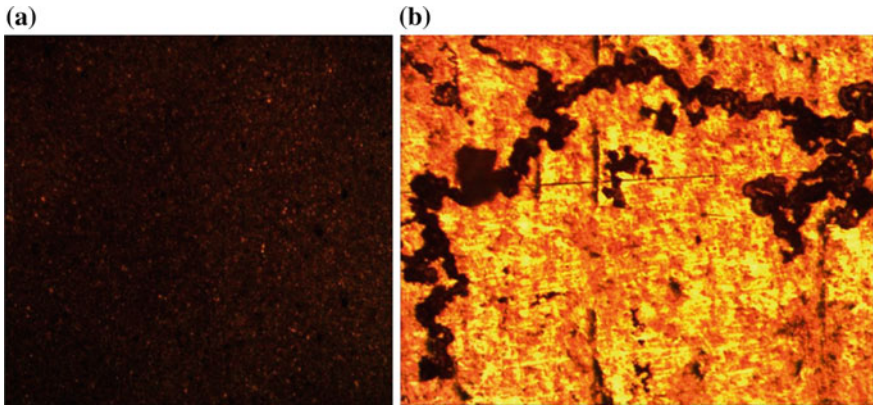
Fig. 2.24 General view of surface of samples made of steel 45 after 3 years of storage in air in ordinary conditions: **a** sample surface with oxide films; **b** unprocessed surface [53]

The research of the piece surfaces (Fig. 2.25a) and of the tool-electrode (Fig. 2.25b) allowed to establish that the latter is also subjected to oxidation. The layer formed on the tool-electrode is discontinuous, with obvious signs of melting and electroerosion. The tool-electrode loses its electrical conductivity properties, changes its original geometry character and requires renewing or cleaning of the active surface during its functioning. For these reasons, the tool-electrode must be made of a material resistant to both electroerosion and oxidation.

The study of the piece surfaces made of steel 45 machined under the oxidation regime by applying PEDM and the analysis of their chemical content allowed to
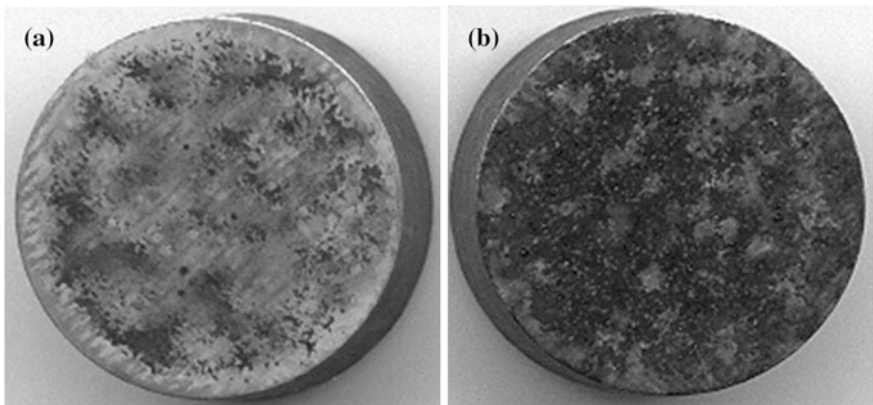

Fig. 2.25 General view of surface of samples made of steel 45 after processing by PEDM (parameters of the processing regime: the charging voltage of the condenser battery $U_c = 140$ V; the capacity of the condenser battery $C = 600$ μF; the gap size $S = 1.5$ mm; the pulse frequency $f = 15$ Hz): **a** cathode- work piece; **b** anode—tool electrode [53]

establish that a considerable percentage of C, N, O, Fe is attested in them
(Figs. 2.16, 2.17, 2.18, 2.19, 2.20 and 2.21, Table 2.1). Among the detected ele-
ments, Fe and C are presented in the base material of the work piece, but O and N
are implanted into the work piece material from the work environment (air). At the
same time, we can say that the result of the surface oxidation processing via PEDM
does not show any significant deterioration of the machined surface. Only
sub-micrometer asperities are attested on it (Fig. 2.22b). The formation of iron
oxides and hydro-oxides in amorphous state was previously attested [32–36, 42, 46,
53–56]. This will be confirmed by corrosion investigations.

The volt-ampere characteristics were plotted for samples with oxidized surfaces
and for those with non-oxidized surfaces based on the investigations of resistance to
corrosion (Fig. 2.26).

If we compare the results presented in Fig. 2.26 we can see that the potential of
anodic dissolution of the sample material has increased to positive values as
compared to the raw sample. With the increase of the voltage applied to the
electrodes, the anodic dissolution process of the investigated samples changes. For
instance, for a voltage U = 2 V the current in the circuit for the raw piece is 300 mA,
while for the sample with oxide films it is about twice lower—161 mA (Fig. 2.27).

Figure 2.27 shows that the volt-ampere characteristics for raw and processed
sample in the range of 1.5–2.5 V are practically similar, which points to the
presence of an isolating film on the surface of the processed sample, that enhances
its active resistance.

Taking into account the previous results [43, 44, 53] aimed at the measurement
of surface active resistance, we might conclude that oxide layers formed on the
surfaces of samples do not have a total continuity. Due to this, their anodic dis-
solution is more intense than it is expected.

In order to determine the corrosion speed, 5 pairs of raw and processed samples
were investigated under the same anodic dissolution (3 % NaCl aqueous solution at
room temperature for steel surfaces, and 30 % H_2SO_4 at the temperature of 80° for

Fig. 2.26 Volt-ampere characteristics of the corrosion process of samples made of steel 45 in electrolyte (3 % NaCl aqueous solution): *1* unprocessed surface; *2* surface with oxide films [53]
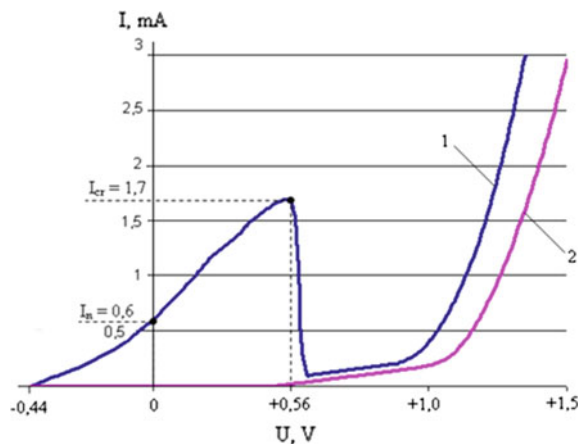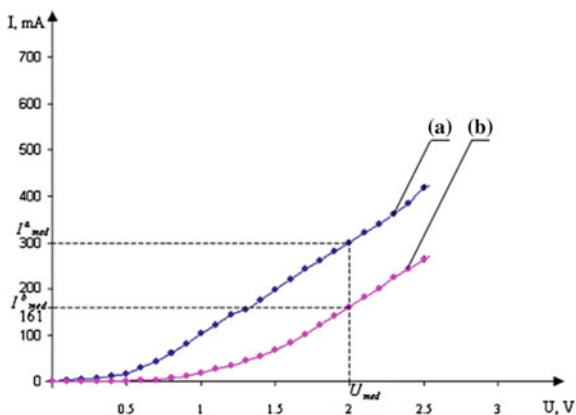
Fig. 2.27 Volt-ampere characteristic of the electro-chemical corrosion process: (*a*) unprocessed surface, (*b*) surface with oxide films [53]

titanium alloy surfaces). The results of measurements are presented in Tables 2.4, 2.5, 2.6 and 2.7.

If we analyze the obtained results, we can conclude that for the processed steel samples the corrosion speed is about twice lower than for unprocessed samples, and it is by about 100 times lower for titanium surfaces.

If we take into account the fact that the natural corrosion potential is tens and hundreds times smaller than in the case of the performed tests, then we can suppose that the efficiency of oxide film application will significantly increase. For instance, if we return to Fig. 2.26, then we can affirm that for applied voltages within 0 and 0.4 V there is no current in the circuit formed by the work piece. Therefore, the

Table 2.4 Speed of anodic dissolution of unprocessed surfaces of samples made of steel 45 [53]

No.	Initial mass of the sample m_i (g)	Final mass of the sample m_f (g)	Δm (g)	Speed of corrosion K (g/m^2 h)
1	12.8441	12.8237	−0.0204	812.10
2	13.1458	13.1254	−0.0204	812.10
3	13.3225	13.3025	−0.0200	796.17
4	14.0610	14.0417	−0.0193	768.31
5	13.0248	13.0031	−0.0217	863.85

Table 2.5 Speed of anodic dissolution of oxidized surfaces of samples made of steel 45 [53]

No.	Initial mass of the sample m_i (g)	Final mass of the sample m_f (g)	Δm (g)	Speed of corrosion K (g/m^2 h)
1	12.8569	12.8441	−0.0128	509.55
2	13.1605	13.1458	−0.0147	585.19
3	13.3338	13.3225	−0.0113	449.84
4	14.0717	14.0610	−0.0107	425.95
5	13.0366	13.0248	−0.0118	469.74

Table 2.6 Speed of anodic dissolution of unprocessed surfaces of samples made of titanium alloy BT8 [53]

No.	Initial mass of the sample m_i (g)	Final mass of the sample m_f (g)	Δm (g)	Speed of corrosion K (g/m² h)
1	1.6803	1.6700	−0.0103	103
2	1.6700	1.6599	−0.0101	101
3	1.6599	1.6466	−0.0133	133
4	1.6466	1.6324	−0.0142	140
5	1.6324	1.6198	−0.0126	126

Table 2.7 Speed of anodic dissolution of oxidized surfaces of samples made of titanium alloy BT8 [53]

No.	Initial mass of the sample m_i (g)	Final mass of the sample m_f (g)	Δm (g)	Speed of corrosion K (g/m² h)
1	1.9582	1.9578	−0.0004	4
2	1.6615	1.6613	−0.0002	2
3	1.8829	1.8828	−0.0001	1
4	1.8325	1.8324	−0.0001	1
5	1.7648	1.7647	−0.0001	1

corrosion speed is zero. However, a considerable current is attested in the same conditions for unprocessed pieces. Therefore, the speed of corrosion is also significant. Finally, we can admit that the application of oxide films on metal surfaces via PEDM is beneficial for enhancing their active resistance, as well as for anti-corrosion protection.

2.7 Conclusions

1. The physical model of the plasma channel interaction with the work piece surface via "cold" electrode spots explains the nanometer diffusion processes in the processed surface strata and can provide a substantial scientific contribution to developing new technologies for the modification of chemical composition of surfaces with their amorphization at nanometer depths;
2. The abnormal diffusion of oxygen in the metal piece surfaces accompanied by the oxide and hydroxide phase formation is due to ozone synthesis in the PEDM plasma, and also to high intensity of the electric field in the anodic and cathodic zones of 10^6–10^8 V/m, high temperatures of 10^4K in the electrode spots, and their short lifetime;
3. During surface machining of samples made of alloys of iron, copper, aluminum and titanium by applying PEDM under ordinary conditions, the surface oxidation is more effective when the workpiece is connected in the discharge circuit

as cathode; this is due to lower voltage drops in this situation and less intensive processes of vaporization of machined surfaces in this technological variant;

4. The layer thickness obtained at surface oxidation via PEDM for samples made of metal alloys depends on the physico-mechanical properties of the base material, on the energy density released in the gap, on the duration of PEDM, and on the number of discharges per unit of the machined surface;

5. The nanometer thickness of the oxide and hydroxide films places this process among nanotechnologies, ensuring simplicity of technology realization and possibilities of processing various materials from the class of metals and semiconductors;

6. The developed technology ensures the increase of the active surface resistance of pieces made of metal alloys by about 10^7 times, the increase of the corrosion potential to positive values (for iron alloys from -0.44 to $+0.4$ V; for titanium alloys from -0.56 to $+0.22$ V) and the decrease of the corrosion speed in the chemically aggressive solutions (for iron alloys by about 2 times and for titanium alloys by about 10^2 times).

References

1. E. Monaico, I. Tiginyanu, Nanowires and nanotubes: technologies and perspectives for their use. Phys. Mod. Technol. **10**(1–2), 4–12 (2012)

2. M. Enachi, O. Lupan, T. Braniste, A. Sarua, L. Chow, Y.K. Mishra, D. Gedamu, R. Adelung, I. Tiginyanu, Integration of individual TiO_2 nanotubes in the chip: nanodevice for hydrogen sensing. Phys. Status Solidi: Rapid Res. Lett. **9**(3), 171–174 (2015)

3. M. Enachi, O. Lupan, T. Braniste, A. Sarua, R. Adelung, I. Tiginyanu, Hydrogen nanosensor based on a single nanotube of TiO_2, in *International Conference on Microelectronics and Computer Science*, October 22–25 Oct 2014, Chisinau, Moldova (2014)

4. O. Lupan, T. Pauporte, I.M. Tiginyanu, V.V. Ursaki, V. Sontea, L.K. Ono, B.R. Cuenya, L. Chow, Comparative study of hydrothermal treatment and thermal annealing effects on the properties of electrodeposited micro-columnar ZnO thin films. Thin Solid Films **519**(22), 7738–7749 (2011)

5. A.I. Hochbaum, R. Chen, R.D. Delgado, W. Liang, E.C. Garnett, M. Najarian, A. Majumdar, P. Yang, Enhanced thermoelectric performance of rough silicon nanowires. Nature **451**, 163–167 (2008)

6. A.I. Boukai et al., Silicon nanowires as efficient thermoelectric materials. Nature **451**, 168–171 (2008)

7. P. Topala, Research on obtaining deposit layers of metal powder by applying pulsed electrical discharge machining. Summary of PhD thesis, Bucharest, University Politehnica (1993), 32 pp

8. V.E. Bulat, M.H. Esterliv, Cleaning metal articles from scale, oxided pellicle and soiling by electro arc discharge in vacuum. FHOM **3**, 49–53 (1987)

9. B.A. Artamonov et al., *Electro-physical and electrochemical methods of material processing*, vol. 1 (Vyssaia Shkola, Moscow, 1983)

10. P.S. Gordienko et al., RF Patent No. 2283901. Technique of electrolytic oxidation of valvular metals and their alloys. Publ. 20.09.2006. Bulletin of inventions No. 28 (2006)

11. Sh Ramanathan, *Thin Film Metal-Oxides. Fundamentals and Applications in Electronics and Energy* (Springer, New York, 2010). 337 p

12. J. Wu, J. Cao, W.-Q. Han, et al., *Functional Metal Oxide Nanostructures* (Springer, New York, 2012), 368 pp

13. Ph Avoris et al., AFM-tip-induced and current-induced local oxidation of silicon and metals. Appl. Phys. A **66**, 659–667 (1998)

14. IYa. Mittova, Ya., Pshestanchik V. R. The chemistry of processes which create dielectric layers with functional group substituents on semiconductors by impurity thermo-oxidation. Russ. Chem. Rev. **60**(9), 967–979 (1991)

15. K. Kushida-Abdelgafar et al., Integr. Ferroelectr. **13**, 113 (1997)

16. K. Shoji, et al., *Symposium on VLSI Technology Digest of Technical Papers* (Widerkehr and Associates, Gaithersburg, 1996), p. 28

17. K. Kushida-Abdelgafar et al., Mechanism of TiN barrier-metal oxidation in a ferroelectric random access memory. J. Mater. Res. **13**(11), 3265–3269 (1998)

18. B. Schmidt, K. Wetzig, *Ion Beams in Materials Processing and Analysis* (Springer, 2013), 418 pp

19. L. Slatineanu, *Non-Conventional Technologies in Machine Building* (Tehnica Info, Chisinau, 2000), p. 252

20. S.S. Ushakov, et al., *Micro-Arc Oxidation of Pipes and Shipbuilding Components Made of Titanium Alloys* (Manual RD5. AEIS. 2459-2006. Saint-Petersburg: FSUE CRI KM "Prometey", 2006), 242 pp

21. I.I. Chernenko, L.A. Snejko, I.I. Papanova, Getting coating by means of anode-spark electrolysis, L. Himia (1991), 128 pp

22. V.V. Nemoshkalenco, et al., Peculiarities of surface strata formation at spark discharge. Kiev: Metal-Phys. **12**(3), 132–133 (1990)

23. P. Levitz, G. Calas, D. Bonin, Etude par spectroscopie Mösbauer du fer (III) dans verres silicates multicomposants d'intérêt géologique. Phys. Appl. **15**, 1169–1173 (1980)

24. P.S. Gordienko et al., Formation of coatings on valvular metals and alloys in electrolytes with capacitive energy control at micro-arcwise oxidation. Prot. Met **42**(5), 500–505 (2006)

25. P. Topala, P. Stoicev, Technologies of conductible material processing by applying pulsed electrical discharge machining. Chisinau: Edition Tehnica-Info (2008), 265 pp

26. I.A. Chapligina (ed.), *Nano technologies*. (Tehnosphere, Moscow, 2013)

27. J. Martin, *The Concise Encyclopedia of Materials Processing* (Elsevier, New York, 2009), 854 pp

28. P. Topala, *Conditions of Thermic and Thermo-Chemical Superficial Treatment Innards with the Adhibition of Electric Discharge in Impulses. Nonconventional Technologies Review* (Editura BREN, Bucureşti, 2005), pp. 27–30

29. P. Topala, Research on obtaining deposit layers of metal powder by applying pulsed electrical discharge machining. PhD thesis, Bucharest, University Politehnica (1993), 161 pp

30. I.I. Safronov, P.A. Topala, A.S. Gorbunov, *Electro-Erosive Processes on Electrodes and the Microstructural and Phase Composition of the Alloy Stratum* (Tehnica-Info, Chisinau, 2009)

31. P.V. Gavrilo,v et al., Microarc oxidation of the working surface of technologically equipped elements made of aluminium alloys. Technologies of repairing, restoration and consolidation of machine pieces, mechanisms, equipment, instruments and technological equipping. Part 2, in *Materials of 9th International Practical Conference*, 10–13 April 2007. Polytechnical University Publishing House, (2007), pp. 77–79

32. P. Topala, A. Ojegov, *Formation of Oxide Thin Pellicles by Means of Electric Discharges in Pulse*. Annals of the Oradea University. Fascicle of Management and Technological Engineering, vol. VII (XVII) (CD-ROM Edition. Editura Universității din Oradea, România, 2008), pp. 1824–1829. ISSN 1583-0691, CNCSIS Clasa B+

33. P. Topala, A. Ojegov, *Formation of oxide Thin Pellicles by Means of Electric Discharges in Pulse* (Buletinul Institutului Politehnic Iași. Tomul LIV (LVIII), 2008), pp. 121–128

34. P. Topala, A. Ojegov, *Formation of Oxide Thin Pellicles by Means of Electric Discharges in Pulse*. Annals of Oradea University. Fascicle of Management and Technological engineering, vol. VII (XVII) (2008), p. 309

35. P. Topala, A. Ojegov, Protection the *Interior Cylindrical Surfaces of Industrial Pipes with Oxide Films Obtained by Applying Pulsed Electrical Discharge Machining*, vol. 21 (State Agrarian University from Moldova. Scientific Papers, Chisinau, 2008), pp. 171–174

36. P. Topala, P. Stoicev, A. Ojegov, Experimental investigations on microoxidation of surfaces by means of applying electrical discharges in impulse under ordinary conditions, in *Creativity Management International Conference—New Face of TCMR*. 21–23th May 2009 (Culegeri de lucrări științifice. Ediția XIII-a. Editura U.T.M., Chișinău, 2009), pp. 172–175

37. L.P. Kornienco et al., Electro-chemical and corrosive behaviour of titanium with electro-spark coating Pd и Cr-Pd. Metal Protect. Moscow **29**(3), 351–358 (1991)

38. P. Topala et al., The influence of tempering on the corrosive behaviour of titanium with electro-spark coating. Metal Protect. Moscow **26**(3), 433–437 (1990)

39. S. Gutt, G. Gutt, *Chemistry of Electro-technical Materials*. Course. University Ştefan cel Mare, Suceava. Romania, (1992), 304 pp

40. M.K. Mitskevich et al., *Electro-erosion Processing of Metals* (Science and Technics, Minsk, 1988), p. 216

41. P. Topala, *The Energy Distribution in the Gap at the Gap Tehnological Appling of the Electrical Discharges in Impulses*. Nonconventional Tehnologies Review, vol. 1. (Editura PIM, Iași, 2007), pp. 129–132

42. V. Besliu, P. Topala, A. Ojegov, Predicting the thickness of the surface layer subjected to applying EDI using modeling through the method of neuronal model. Machine building and tehno-sphere of XXI century, in *Materials of XVIth International Scientifico-Technical Conference*, Sebastopol, September 14–19 2009, Donetsk: DonNTU, vol. 4 (2009), pp. 30–34

43. P. Topala, P. Stoicev, A. Ojegov, N. Pinzaru, E. Monaico, Analysis of processes occurring on the tool and piece electrode surface during the formation of by applying electrical discharges in impulse, in *ModTech 2010*, 20–22 May 2010. Slănic-Moldova, România, (2010), pp. 631–634

44. P. Topala, P. Stoicev, A. Ojegov, N. Pinzaru, Effects of abnormal dissolving of oxygen in metals under the influence of electrical discharges in impulse plasma. Int. J. Mod. Manuf. Technol. **2**, 95–102 (2010). ISSN 2067-3604

45. A. Ojegov, *The Action Of Electrical Discharges in Impulse Plasma on Structure and Properties of Steel 45 Surface Strata*. Engineering Meridian, vol. 4. Edition U.T.M. (2010), pp. 44–47

46. P.A. Topala, P. Vizureanu, A.V. Ojegov, P.N. Stoichev, M.K. Perju, Some results of metal surface microoxidation by means of electropulsed discharges, in Materials of 13th Scientifico-Practical Conference Technologies of Repairing, Restoration and Consolidation of Machine Pieces, Mechanisms, Equipment, Instruments and Technological Equipping, St. Petersburg, 12–15 April 2011, pp. 1087–1094

47. C.C. Kao, J.A. Shih, Sub-nanosecond monitoring of micro-hole electrical discharge machining pulses and modeling of discharge ringing. Int. J. Mach. Tools Manuf. **46**, 1996–2008 (2006)

48. P. Pecas, E. Henriques, Electrical discharge machining using simple and powder-mixed dielectric: the effect of the electrode area in the surface and topography. J. Mater. Process. Technol., 1–9 (2007)

49. Y. Li et al., Micro electro discharge machine with an inchworm type of micro feed mechanism. J. Int. Soc. Precis. Eng. Nanotechnol. **26**, 7–14 (2002)

50. Y. Uno et al., A new polishing method of metal mold with large-area electron beam irradiation. J. Mater. Process. Technol. **187–188**, 77–80 (2007)
51. A. Hirbu, P. Topala, A. Ojegov, Auto-ionization laboratory plasma, in *ModTech International Conference "Modern Technologies in Industrial Engineering*, Book of abstracts, June 27–29, 2013, Sinaia, Romania (2013), p. 359
52. A. Hirbu, P. Topala, A. Ojegov, Laboratory plasma formation without preventive ionisation of the active medium, in *The 17th International Salon of Research and Technological Transfer* "INVENTICA 2013", (2013), pp. 721–722
53. A. Ojegov, Obtaining thin oxide films on metal surfaces of iron, copper, aluminum and titanium alloys, by applying pulsed electrical discharge machining. Summary of PhD thesis in technique. Edition "Tehnica UTM", Chisinau (2014), 32 pp
54. P. Topala, A. Hirbu, A. Ojegov, New directions in the practical application of electro erosion, in *Annual Session of Scientific Papers IMT* Oradea—2011, Oradea, Felix Spa, May 26–28th, 2011, sect. Tehnologia Construcţiei de Maşini. Annals of the Oradea University. Fascicle of Management and Technological Engineering (2011)
55. P. Topala, A. Hirbu, A. Ojegov, *New Directions in the Practical Application of Electro Erosion*. Nonconventional Technologies Review, vol. 1 (2011), pp. 49–56
56. P. Topala, V. Besliu, V. Rusnac, A. Ojegov, N. Pinzaru, Structural modification of the chemical composition and microgeometry of the piece surfaces by applying pulsed electrical discharge machining. *Physics and Technics: Processes, Models, Experiments*, vol. I. (Balti University Press, Balti, 2011), pp. 36–42
57. P. Topala, V. Rusnac, V. Beşliu, A. Ojegov, N. Pînzaru, Physical and chemical effects of EDI processing. Int. J. Eng. Technol. **2**(1), 6 http://www.i-jet.eu/journal_ijet/c_p_ijet1112.pdf
58. A. Ojegov, The influence of pulsed electrical discharge machining parameters on the intensity of oxide films formation on steel 45 surface. Phys. Mod. Technol. **10**(3–4), 18–24 (2012)
59. P. Topala, A. Ojegov, About chemical and phase content of nano-pellicles formed on metal surfaces by applying electrical discharges in impulse, in *Proceedings of International Scientific Conference* "*10 years of Nanotehnology Development in the Republic of Moldova*", 22—23 Oct 2012, Balti, (2012), p. 21
60. P. Topala, V. Besliu, P. Stoicev, A. Ojegov, Application of electric discharges in impulse in micro and nano-technology, in *Proceedings of the 16th International Conference Modern Technologies, Quality and Innovation—New face of TMCR,* vol. II, 24–26 May, 2012, Sinaia, Romania, (2012), pp. 969–972
61. P. Topala, D. Luca, A. Ojegov, P. Stoicev, N. Pinzaru, Results on metal surface nano-oxidation by electrical discharges in impulse, in *ICCCI 2012. The Fourth International Conference on The Characterization and Control of Interfaces for High Quality Advanced Materials. Kurashiki, Japan*, 2–5 Sept 2012. (2012), p. 85
62. P. Topala, A. Ojegov, V. Besliu, Oxygen diffusion during the formation of thin pellicles by applying EDI, in *ModTech International Conference "Modern Technologies in Industrial Engineering"*, Book of abstracts, June 27–29, 2013, Sinaia, Romania, (2013), 356 pp
63. M. Yang, et al., Scanned probe oxidation on an octadecyl-terminated silicon (111) surface with an atomic force microscope: kinetic investigation in line patterning. Nanotechnology **17**, 330–337 (2006)
64. Ph Avoris et al., Atomic force microscope tip-induced local oxidation of silicon: kinetics, mechanism, and nanofabrication. Appl. Phys. Lett. **71**(2), 285–287 (1997)
65. W. Mönch, *Semiconductor Surfaces and Interfaces* Springer (Ser. Surf. Sci.), vol. 26, Chap. 17, (1993), 276 pp
66. Y. Nishioka, et al., *Proceedings of 1995 International Electron Devise Meeting* (1995), p. 903
67. A.V. Ancudinov, et al., Nano-relief of the oxidated surface of the railings of alternated heterostrata $Ga_{0.7}Al_{0.3}As$ и GaAs. Phys Technol. Semicond. **33**(5), 594–597 (1999)
68. S.A. Kovaleva, et al., Morphology and structure of silicon oxide anodic pellicles obtained by means of probe oxidation using the atomic power microscope. Nano Technologies Popnano RU/HIOKR/ Investigations (2008)

69. D.V. Sokolov, Mechanisms of n-In GaAs nano-oxidation with the use of atomic force microscope. JTPh **72**(1), 60–65 (2002)
70. P. Topala, A. Ojegov, V. Besliu, A. Hirbu, N. Pinzaru, MD Patent No. 4325. Multi-electrode tool for surface pulsed electrical discharge machining. Natalia. Publ. 28 Feb 2015